DYNAMIC CONTROL OF HYDROGEL PROPERTIES

VIA ENZYMATIC REACTIONS

A Thesis

Submitted to the Faculty

of

Purdue University

by

Dustin M. Moore

In Partial Fulfillment of the

Requirements for the Degree

of

Master of Science in Biomedical Engineering

May 2019

Purdue University

Indianapolis, Indiana

THE PURDUE UNIVERSITY GRADUATE SCHOOL
STATEMENT OF THESIS APPROVAL

Dr. Chien-Chi Lin, Chair

     Department of Biomedical Engineering

Dr. Dong Xie

     Department of Biomedical Engineering

Dr. Jiliang Li

     Department of Biology

Approved by:

     Dr. Julie Ji

          Head of the Graduate Program

ACKNOWLEDGMENTS

I would like to acknowledge my thesis advisor, Dr. Chien-Chi Lin, for his guidance, assistance, and support throughout this research and thesis work. Dr. Lin has given me plenty of opportunities to further my research skills and has taught me many new techniques in the lab, in professional writing, and in the presentation of research. I will always be grateful for the professional development that he has provided for me.

I would also like to thank my advisory committee members, Dr. Dong Xie and Dr. Jiliang Li, for their time and input throughout this thesis work.

I would also like to thank my current and past colleagues: Mr. Hung-Yi (Gino) Liu, Mr. Matthew Arkenberg, Mr. Kevin Peuler, Ms. Han Nguyen, Mr. Hunter Johnson, Ms. Britney Hudson, Mr. Jon Stoller, and Mr. Nathan Dimmitt for their support and friendship. I would also like to extend a special thanks to Mrs. Sherry Clemens for all of her support throughout my graduate studies.

TABLE OF CONTENTS

LIST OF FIGURES

LIST OF ABBREVIATIONS

ECM	Extracellular matrix
2D	2-dimensional
3D	3-dimensional
4D	4-dimensional
SrtA	Sortase A
$SrtA_{WT}$	Wild-type Sortase A
$SrtA_{5M}$	Pentamutant Sortase A
$SrtA_{7M}$	Heptamutant Sortase A
PEG	Poly(ethylene glycol)
(h)MSC	(Human) mesenchymal stem cell
MMP	Matrix metalloproteinase
TGF-β	Transforming growth factor-β
IL	Interleukin
IL-RA	Interleukin-receptor antagonist
VEGF	Vascular endothelial growth factor
HGF	Hepatocyte growth factor
PDGF	Platelet-derived growth factor
KGF	Keratin growth factor
TIMPs	Tissue inhibitor of metalloproteinases
MeHA	Methacrylated hyaluronic acid
DTT	Dithiothreitol
PETMA	Pentaerythritol tetrakis (mercaptoacetate)
UV	Ultraviolet
HA	Hyaluronic acid

DTPA	Diethylenetriaminepentaacetic acid
DBCO	Dibenzylcyclooctyne
SPAAC	Strain-promoted azide-alkyne cycloaddition
GelNB	Norbornene functionalized gelatin
(h)iPSC	(Human) induced pluripotent stem cell
HCC	Hepatocarcinoma cells
HNE	Human neutrophil elastase
BSA	Bovine serum albumin
PLGA	Poly(lactic-co-glycolic acid)
EGF	Epidermal growth factor
MT	Mushroom tyrosinase
NB	Norbornene
DCC	N,N-dicyclohexylcarbodiimide
DMAP	4-(dimethylamino)pyridine
HBTU	N,N,N,N-tetramethyl-O-(1H-benzotriazol-1-yl)uranium hexafluorophosphate
HOBt	Hydroxybenzotriazol
IPTG	Isopropyl-D-1-thiogalactopryanoside
MBTH	3-methyl-2 benzothiazolinone hydrazone hydrochloride monohydrate
E. Coli	Escherichia coli
LB	Lysogeny broth
ddH$_2$O	double distilled water
TFA	Trifluoroacetic acid
TIS	Triisopropylsilane
LAP	Lithium phenyl-2,4,6-trimethylbenzoylphosphinate
DMEM	Dulbecco's modified eagle medium
FBS	Fetal bovine serum
bFGF	Basic fibroblast growth factor

(D)PBS   (Dulbecco's) phosphate buffered saline

ANOVA   Analysis of variance

DOPA   Dihydroxyphenylalanine

LIST OF NOMENCLATURE

G'	Storage modulus
$W_{Dry,1}$	Dry weight 1
$W_{Dry,2}$	Dry weight 2
$W_{Swollen}$	Swollen weight
Q_m	Mass swelling ratio
Q_v	Volumetric swelling ratio
ρ_1	Solvent density
ρ_2	Polymer density
$\overline{\nu}$	Specific volume of the polymer
ν_1	Molar volume of solvent
ν_2	Polymer volume fraction
C_n	Flory characteristic number
$\overline{M}_n$	Molecular weight of polymer
$\overline{M}_c$	Average molecular weight between crosslinks
$(\overline{r_0^2})^{\frac{1}{2}}$	Root-mean-squared end-to-end distance between two crosslinks
l	Average bond length in polymer
$X_{1,2}$	Polymer-water interaction coefficient
ξ	Mesh size

ABSTRACT

Moore, Dustin M. M.S.B.M.E., Purdue University, May 2019. Dynamic Control of Hydrogel Properties via Enzymatic Reactions. Major Professor: Chien-Chi Lin.

Dynamic changes to the extracellular matrix (ECM) impact many cell fate processes. The ECM can experience changes in stiffness as well as changes in composition in response to injury, development, and diseases. To better understand the role that these dynamic processes have on the cells residing within the environment, researchers have turned towards 4-dimensional (4D) hydrogel designs. These 4D hydrogels re-capitulate not only 3-dimensional (3D) matrix architectures, but also temporal changes in the physicochemical properties. The goal of this thesis was to design a unify chemistry (i.e., Sortase A (SrtA)-mediated transpeptidation) for dynamic tuning hydrogel stiffness and the presence of bioactive ligands. The first objective was to establish a tunable and cytocompatible enzymatic scheme for softening cell-laden hydrogels. Briefly, the effects of SrtA-mediated matrix cleavage were investigated using poly(ethylene glycol) (PEG)-peptide hydrogels crosslinked by SrtA-sensitive and insensitive peptides. Initially, the effects of various parameters with respect to catalytic reactions of SrtA were characterized rheologically, including enzyme and substrate concentrations, macromer content, peptide composition, and treatment time. Gel moduli pre- and post-enzyme treatment were measured to verify SrtA-mediated hydrogel softening. The cytocompatibility of SrtA-mediated gel softening system was investigated using human mesenchymal stem cell (hMSC). Upon treatment with SrtA and an oligoglycine substrate, encapsulated hMSCs exhibited extensive spreading in comparison to those within statically stiff matrices. The second objective was to establish a reversible ligand exchange system utilizing SrtA-mediated transpeptidation. SrtA-sensitive pendant ligands were immobilized within PEG hydrogels, which were

treated with SrtA and an oligoglycine substrate to afford tunable removal of the pendant ligand. Through measurement of the liberated pendant peptide concentration, it was found that higher concentrations of SrtA or extending treatment times led to higher ligand removal efficiency. Finally, the effect of peptide ligand removal on cell behaviors were evaluated using NIH 3T3 fibroblasts. Fibroblasts were culture both on and within hydrogels containing SrtA-cleavable cell adhesion peptide. After treatment, both conditions led to a decrease in fibroblast spreading in comparison to non-treated gels. Overall, the utility of SrtA as versatile agent for controlling the mechanical properties and the presence of biologically active components within a hydrogel system was demonstrated. These systems could be further explored with natural-based materials to better mimic the physiological environment experienced by cells.

CHAPTER 1. INTRODUCTION

1.1 Dynamic Biological Systems and Their Role in Stem Cell Fate

Biological tissues are composed of extracellular matrices (ECM) that undergo dynamic changes in stiffness, ligand presentation, viscoelasticity, and availability of soluble signaling molecules. These environmental cues influence morphology, growth, and differentiation potential of the cells residing in the tissue [1–6]. For example, mesenchymal stem cells (MSCs) have been shown to change their lineage commitment when exposed with different matrix stiffness [4,7] and cell adhesive molecules [8]. In general, cells can remodel their environments through secretion of proteases such as matrix-metalloproteinases (MMPs) or matrix proteins (e.g., fibronectin, collagen, and proteoglycans). Through the secretion of MMPs, cells can degrade and soften the local matrix. On the other hand, deposition/removal of matrix proteins can induce changes in intracellular signaling. These dynamic processes can play a significant role in altering a stem cells fate.

1.1.1 Dynamics of Wound Healing

Wound healing is an example of a natural biological process involving dynamic changes in local stiffness, growth factors, and ECM composition. There are three main stages seen in wound healing: inflammation, proliferation, and remodeling. During the inflammation stage, an increase in cytokines leads to the localization of inflammatory cells such as macrophages and neutrophils, while platelet aggregation leads to clotting at the site of the wound. These inflammatory cells scour the region

and uptake foreign materials and damaged cells to clean out the site. These cells also secrete growth factors which become immobilized within the ECM. In the proliferation stage, fibroblasts invade the wound site and secrete ECM proteins, much of which is collagen III rich. This temporary structure is often called the provisional matrix. The increase of collagen content allows for more fibroblast-ECM interactions through integrin binding and formation of focal adhesion complexes that trigger mechanotransduction in the cells. Increased matrix stiffness promotes activation of myofibroblasts, which exert contractile forces within the matrix leading to its increased rigidity. Contraction induced by myofibroblasts also facilitates the release of various growth factors, such as transforming growth factor-β1 (TGF-β1), that were otherwise trapped within the ECM [9]. During this stage, the tissue also experiences hypoxic conditions, which activates angiogenesis to allow for the formation of new blood vessels within the fibrotic region. The release of cytokines and the increase in collagen promotes re-epithelization, ultimately leads to proliferation and migration of epithelial cells to cover the wound. The high collagen content mediates increased adhesion by epithelial cells, which promotes intracellular mechanotransduction. After a few days, remodeling begins, in which collagen III deposited by fibroblasts is gradually degraded and collagen I is secreted to take its place. Other ECM proteins are also deposited to return the tissue to its natural composition as seen prior being damaged. The degradation of the provisional matrix coincides with ECM softening [10–13].

Various studies have looked into the roles of MSCs in the three phases of wound healing [14–16]. Within the inflammation stage, MSCs regulate the inflammatory response through the secretion of anti-inflammatory cytokines interleukin-10 (IL-10) and IL-4 [14]. MSCs have also been seen to play a role in managing the immune response within injured tissue through the secretion of factors such as IL6, TGF-β, and inerleukin-1 receptor antagonist (IL-1RA), to name a few [15]. Within the proliferative stage, MSCs have been seen to secrete pro-migratory and proliferative growth factors such as vascular endothelial growth factor (VEGF), hepatocyte growth factor (HGF), and platelet derived growth factor (PDGF) [14, 16]. These factors

promote vascularization as well as infiltration of endothelial cells, fibroblasts, and keratinocytes. In the remodeling stage, MSC release TGF-β3 as well as keratin growth factor (KGF) while also regulating MMPs and tissue inhibitor of metalloproteinases (TIMPS) [14]. Overall, MSCs take on an important role in regulating the wound healing process.

1.2 Designing Biomimetic Matrices for Culturing Cells

The dimensionality of the matrix in which cells are cultured in has been shown to have a significant impact on their morphological and signaling properties [7]. In two-dimensional (2D) culture environments, MSCs spread more as the stiffness of the substrate increases. In three-dimensional (3D) environments, the opposite was found to be true, as MSCs adopted a more spherical morphology within stiffer matrices while spreading in softer matrices [17]. As cells often reside within 3D environments, researchers have designed various 3D scaffolds to better recapitulate the natural microenvironments in the ECM. Hydrogels are commonly used due to their high water content, ability to incorporate biomimetic motifs (for cellular adhesion, degradation, etc.), and tunability of various mechanical properties. Hydrogels have been created from a multitude of synthetic (PEG) and natural materials (gelatin, hyaluronic acid, etc.). Recently, the focus has evolved to designing dynamic hydrogel systems that can mimic changes in stiffness as well as to allow for the introduction or removal of bioactive agents [18–20].

1.2.1 Softening Hydrogel Matrix

Recently research has focused on designing hydrogels which mimic the dynamic changes in stiffnesses seen in natural tissue. Hydrogels can be designed to undergo temporal degradation through hydrolysis [21, 22], photo-lysis [23–25], and proteolysis [26, 27]. Burdick and colleagues crosslinked methacrylated hyaluronic acid (MeHA) with dithiothreitol (DTT) and pentaerythritol tetrakis(mercaptoacetate) (PETMA).

The PETMA structure contains hydrolytically degradable ester motifs. PETMA containing gels could be gradually softened from an elastic modulus of 17 kPa to 3 kPa over the course of two weeks [21]. Nonetheless, hydrolytic degradation is a slow process. In this regard, photolabile linkers have been integrated within hydrogel networks to permit real-time and spatiotemporally controllable degradation. For example, Anseth and colleagues have designed a hydrogel system crosslinked by PEG-acrylate containing photolabile nitrobenzyl ether motifs. Introduction of ultraviolet (UV) light led to the degradation of these linkages. Through the use of a photomask, the hydrogels could be spatially softened on demand [23]. In another example, Stowers et al. demonstrated a liposome loaded alginate hydrogel system that could be stiffened or softened through near infrared light exposure. Briefly, ionically crosslinked alginate hydrogels were formed with encapsulated liposomes containing gold nanorods and either calcium chloride or with calcium-chelating diethylenetriaminepentaacetic acid (DTPA). Upon exposure to 808 nm light, the gold nanorods would radiate heat to increase the permeability of the liposomes. Calcium chloride released from these liposomes facilitated further ionic crosslinking of the alginate gels, hence leading to matrix stiffening. On the other hand, release of DTPA would lead to the chelation of calcium ions, in turn softening the hydrogels [24].

1.2.2   Reversible Softening of a Hydrogel Matrix

Reversibly softenable hydrogels have also been of interest due to their ability to mimic the dynamic matrix mechanics observed in normal physiological processes (e.g., wound healing). Burdick and colleagues designed hyaluronic acid (HA) hydrogels crosslinked by thiol-acrylate nucleophilic crosslinking. These HA hydrogels could be softened owing to the incorporation of photolabile o-Nitrobenzyl linker when exposed to UV (365nm) light. On the other hand, the methacrylates in the HA hydrogel network enabled a secondary photopolymerization (400-500nm light) to increase the network crosslinking density [28].

Rosales et al. took advantage of azobenzene photoisomerization in conjunction with azobenzene/β-cyclodextrin guest-host interactions to produce a hydrogel with reversible softening capability. Uniquely, β-cyclodextrin formed a strong non-covalent interaction with the trans isomer of azobenzene but not with its cis conformation. Azobenzene was transitioned from a cis conformation to a trans conformation through exposure to 365nm and 400-500nm light, respectively. Guest-host gels were formed using azobenzene-functionalized and β-cyclodextrin-functionalized HA. Softening was achieved by exposing gels to 365nm light to convert azobenzene to its cis conformation. Gels were then able to be re-stiffened upon treatment with 420nm light to change azobenzene back to its trans conformation. Reversible softening and re-stiffening could be cyclically repeated [25].

1.2.3   Ligand Addition and Removal

To further mimic the dynamic conditions of natural tissue, techniques have been introduced to permit the exchange of bioactive ligands into and out of hydrogel systems. Some chemistries have demonstrated the ability to either add or remove specific ligands into a system on demand, but few have been capable of dynamically adding and removing ligands repeatedly. One example of the introduction of a ligand on demand was demonstrated by Cosgrove et al. through the immobilization of integrin-binding RGD as well as a cadherin binding HAVDI peptide sequences through the use of photo-initiated thiol-methacrylate Michael-type addition [29]. The addition of HAVDI regulated MSC contractility, effectively altered cell fate. Other techniques utilized photochemistries to immobilize ligands post-gelation immobilization of ligands within a network, including thiol-methacrylate reactions [20].

Anseth and colleagues synthesized a photolabile nitrobenzyl ether linker containing RGD to allow for cleavage of cell adhesion motif via UV light irradiation [23]. Through the use of this technique, they demonstrated that removal of RGD promoted chondrogenic differentiation of hMSCs. Grim et al. investigated the use of

a reversible thiol-ene chemistry for on-demand and spatially-controllable ligand exchange through exposure to light [30]. Allyl sulfide motifs were incorporated within PEG-dibenzylcyclooctyne (DBCO) PEG-azide gels formed by strain-promoted azide-alkyne cycloaddition (SPAAC). When exposed with UV (365nm) light and a photoinitiator, lithium phenyl-2,4,6-trimethylbenzoylphosphinate (LAP), the allyl sulfide motifs were able to reversibly react with molecules containing free thiol. Grim was able to spatially immobilize two thiolated proteins within the same matrix. This was achieved by first incubating and UV treating the gel with thiolated ovalbumin, and then subsequently incubating with thiolated transferrin and UV treating [30]. Transferrin was replaced within the gels by PEG-thiol upon UV treatment.

1.3 Enzyme-Responsive Hydrogels

Enzymes have often been utilized within hydrogel systems due to their specificity and cytocompatibility. By incorporating MMP-sensitive motifs within crosslinks, cells are able to locally degrade the polymer matrix. This allows for cell-mediated spreading and local softening of the surrounding matrix [31, 32]. By selectively including peptide motifs sensitive to specific MMPs, degradation can be cell-type specific [33, 34]. Anseth and colleagues demonstrated the use of cell-mediated cleavage as a means of controlling available cell adhesion ligand within a hydrogel system. hMSC-laden PEG thiol-norbornene hydrogels were created with the inclusion of RGD with or without a linked MMP-sensitive sequence. Cell-secreted MMP led to the cleavage of MMP-linked RGD from the gels, which promoted chondrogenic differentiation of encapsulated hMSCs [35]. Liang et al. were able to soften hepatocarcinoma cell (HCC)-laden PEG-crosslinked collagen hydrogels from an elastic modulus of 4 kPa to 0.5kPa by introducing soluble MMP-1. HCC cells grown within the MMP-softened gels formed larger spheroids and were more sensitive to radiation treatment in contrast to spheroids grown in non-treated stiff gels [26].

Chymotrypsin is another cell-secreted protease that has been utilized in hydrogel softening [36] and ligand removal [37]. Plunkett et al. incorporated a bis-cysteine containing chymotrypsin-sensitive peptide (CY↓KC) or inert peptide (CSKC) within thiol-vinyl sulfone crosslinked PEG hydrogels. When treated with -Chymotrypsin, the hydrogels containing the CYKC sequence degraded while the CSKC crosslinked hydrogels remained unaffected [36]. The limitations of utilizing protease-sensitive motifs within hydrogels for user-controlled softening and ligand exchange often arises from the ability for cells to secrete the same proteases.

Human neutrophil elastase (HNE) is another example of a protease which has been utilized in the softening of hydrogels. This protease interacts with proteins and elastin which contain the amino acid sequence Ala-Ala-Pro-Val. Aimetti et al. demonstrated the use of human neutrophil elastase (HNE) in the controllable degradation of PEG hydrogels containing HNE-sensitive (Ala-Ala-Pro-Val/Nva(norvaline)) crosslinker. Degradation of these hydrogels could be controlled by the concentration of HNE, crosslinker composition (Valine vs norvaline), and treatment time. They demonstrated temporally controllable release of bovine serum albumin (BSA) encapsulated within the hydrogels by alternating between 30 minute incubations in a solution with or without HNE [27,38]. They also noted that this degradation occurred via surface erosion. Ashton et al. incorporated alginase loaded poly(lactic-co-glycolic acid) (PLGA) microspheres within ionically crosslinked alginate hydrogels. Release of alginase from the PLGA microspheres, via diffusion, mediated the degradation of hydrogels. This degradation was also tunable by adjusting alginase concentration within microspheres and the microsphere concentration within the hydrogels [39].

1.3.1 The Applicability of the Transpeptidase Sortase A

Sortase A (SrtA) is a cysteine transpeptidase that cleaves peptide substrates with Leu-Pro-X-Thr-Gly (X can be any amino acid except for proline) motif [40–42]. The high specificity of this enzymatic reaction makes it a cytocompatible op-

tion for hydrogel modification [43]. SrtA cleaves the sequence between the Thr and the Gly, forming a thioester intermediate with the Thr and releasing the Gly. This intermediate reacts with any N-terminal Gly containing substrate, allowing for the ligation of two desired molecules. As the product of the reaction also contains the Leu-Pro-X-Thr-Gly substrate motif, this reaction is reversible and can be driven by available secondary substrates containing an N-terminal Gly. In the absence of a glycine substrate, the intermediate can react with water to produce an irreversible LPXT-OH product. Wild-type SrtA (SrtA$_{\mathrm{WT}}$) is calcium dependent. Through genetic engineering, various SrtA mutations have been created to improve its reactivity independent of calcium. For example, a pentamutant SrtA(SrtA$_{\mathrm{5M}}$) (P94R/D160N/D165A/K190E/K196T) was designed to increase the catalytic activity SrtA for up to 140-fold [44]. A SrtA heptamutant (SrtA$_{\mathrm{7M}}$, hereafter referred to as SrtA) (P94R/E105K/E108A/D160N/D165A/K190E/K196T) was designed through introduction of two additional mutations (E105K and E108A), which render the heptamutant calcium-independent through the stabilization of the calcium-binding $\beta6$-$\beta7$ loop [42].
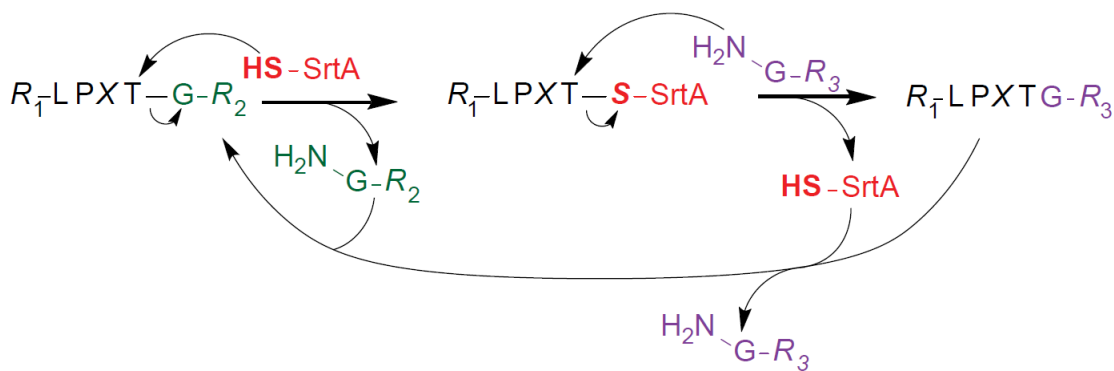
Fig. 1.1: Schematic of the reversible SrtA transpeptidation mechanism.

SrtA has been utilized for many applications including tagging proteins with fluorophores [45] and peptide cyclization [46]. For example, Griffith and colleagues utilized SrtA to immobilize epidermal growth factor (EGF, in the form of GGG-EGF) into PEG hydrogels containing pendant LPRTG [47]. This group also demonstrated

its use in complete degradation of hydrogels created with a crosslinker containing the SrtA-sensitive motif [48]. SrtA has also been utilized to crosslink hydrogels [43, 49]. Recently, Arkenberg et al. implemented SrtA-mediated crosslinking mechanism to form hydrogels that could be subsequently stiffened upon treatment with mushroom tyrosinase (MT) [50]. Since SrtA can catalyze reversible transpeptidation, Arkenberg et al. also demonstrated hydrogels containing pendant LPRTG and GGG peptide could be reversibly stiffened and softened. Specifically, cyclic stiffening and softening was achieved through incubation in solutions containing either SrtA alone or SrtA with an oligoglycine substrate [51]. Due to reversibility of the reaction, SrtA is a very appealing enzyme for introduction and the subsequent removal of substrates on demand.

CHAPTER 2. OBJECTIVES

2.1 Overview

Controllable degradation/softening of hydrogels could be achieved through light-mediated, enzymatic, and hydrolytic reactions. Similarly, techniques have been developed for removal and addition of specific ligands into a hydrogel system. Many of these techniques, however, utilize irreversible or non-specific chemistries. SrtA transpeptidation has been widely utilized in various tagging, immobilization, and conjugation methodologies due to its high specificity and orthogonality. The overarching goal of this thesis was to exploit SrtA for softening and for reversible addition/removal of bioactive molecules within a hydrogel system.

2.2 Objective 1: Establish an Enzyme-Mediated System for Controlled Softening of Cell-Laden Hydrogels

The first objective of this thesis was to utilize SrtA-mediated transpeptidation for on-demand softening of cell-laden hydrogels. To achieve this, PEG-based hydrogels were formed with SrtA-sensitive and insensitive peptide crosslinkers. The gels were crosslinked via photo-click thiol-norbornene chemistry. The softening efficiency of various SrtA and oligoglycine substrate concentrations was investigated. The initial macromer concentration and the ratio of SrtA-sensitive and insensitive peptide sequences within hydrogels was investigated to characterize controllable degrees of softening. The system was then utilized to observe the effects of matrix softening on spreading of encapsulated hMSCs.

2.3 Objective 2: Establish an Enzyme-Mediated System for On-Demand Ligand Exchange

The second objective of this thesis was to utilize the same SrtA-mediated transpeptidation to introduce and/or remove cell-adhesive ligands on demand. Due to the reversible nature of SrtA transpeptidation, this would theoretically allow for repeated ligand exchange. To accomplish this, PEG-based hydrogels were created with an included SrtA-sensitive pendant ligand. The pendant could be removed upon treatment with SrtA and an oligoglycine substrate. The cleaved pendant was then able to be quantified. The effects of SrtA concentration and treatment times on ligand exchange were investigated. To further analyze SrtA-mediated ligand exchange, 3T3 fibroblasts cultured on gels with SrtA-sensitive cell adhesion peptide were treated to remove the bioactive molecule.

CHAPTER 3. MATERIALS AND METHODS

3.1 Materials

Eight-arm PEG-OH (PEG8OH, 20kDa) and four-arm PEG-SH (PEG4SH, 10kDa) were acquired from JenKem Technology. 5-Norbornene-2-carboxylic acid, 2-butanone, N,N-dicyclohexylcarbodiimide (DCC), 4-(dimethylamino)pyridine, lithium bromide, (DMAP), dimethyl phenylphosphonite, tyrosinase, 2,4,6-trimethylbenzoyl chloride, diethyl ether, and isopropyl-D-1 thiogalactopyranoside (IPTG) were obtained from Sigma-Aldrich. Fmoc-protected amino acids, hydroxybenzotriazole (HOBt), and N,N,N,N-tetramethyl-O-(1H-benzotriazol-1-yl)uranium hexafluorphosphate (HBTU) were purchased from Anaspec. 3-Methyl-2 benzothiazolinone hydrazone hydrochloride monohydrate (MBTH) was purchased from Acros Organics. Tyramine hydrochloride was purchased from Chem-Impex International. Glycinamide hydrochloride was obtained from Alfa Aesar. BL21 Escherichia coli (E. coli) was purchased from New England Biolabs. Kanamycin sulfate was obtained from IBI Scientific. Lysogeny broth (LB), Lennox formulation, agar and broth were obtained from DOT Scientific. Mammalian cell Live/Dead staining kit was obtained from Life Technologies Corp. All other chemicals were obtained from Fisher Scientific unless otherwise noted.

3.2 PEG Macromers, Peptide, and LAP Synthesis

Eight-arm PEG-norbornene (PEG8NB) was synthesized as reported with minor modifications to the protocol [52]. 5-norbornene-2-carboxylic acid (5X molar excess to PEG hydroxyl groups) was reacted with DCC (2.5X) in anhydrous DCM for 1 hour to

form norbornene anhydride with a by-product of urea. Urea was filtered out and the remaining norbornene anhydride was added dropwise via an addition funnel to a two-necked round-bottom flask containing PEG8OH, DMAP (0.5X), and pyridine (0.5X) under nitrogen. The reaction occurred overnight at dark. The process was repeated by reacting freshly synthesized norbornene anhydride with the PEG8NB product overnight to further increase norbornene functionalization. The PEG8NB product was recovered via precipitation in cold diethyl ether and vacuum dried overnight. The dried product was redissolved in double distilled H2O (ddH$_2$O) and dialyzed against ddH$_2$O for 3 days at room temperature (MWCO: 6000-8000 kDa), and then lyophilized. ^{1}H NMR (Bruker Advance 500) was used to determine the degree of functionalization ($\sim$85-95%)

Peptides (KCLPRTGCK, KCLPRTACK, GGGGC, KCGPQGIWGQCK, CRGDS, CLPRTGYK, CLPRTGRGDS, and GGGRGDS) were synthesized via Fmoc coupling chemistry in an automated, microwave-assisted peptide synthesizer (Liberty 1, CEM). Crude products were cleaved from the resin with 95% trifluoroacetic acid (TFA), 2.5% ddH2O, 2.5% triisopropylsilane (TIS), and 5% (w/v) phenol at room temperature with stirring for 3 hours. Cleaved peptides were precipitated in cold ethyl ether and vacuum dried overnight. The dried peptide was purified via HPLC (Flexar system, Perkin Elmer) and confirmed via mass spectrometry (QTOF, Agilent Technologies). Peptides were aliquoted in pH 7.4 PBS and stock concentrations measured via the use of Ellmans assay (PIERCE) to quantify free sulfhydryl groups. GGGRGDS was aliquoted directly by molecular weight into 120mM stock solutions.

Photoinitiator lithium phenyl-2,4,6-trimethylbenzoylphosphinate (LAP) was synthesized as previously described [53].

3.3 Heptamutant SrtA Expression and Purification

Heptamutant SrtA (P94R, E105K, E108Q, D160N, D165A, K190E, K196T) was expressed and purified as described previously [50, 54]. Briefly, pet30b-7M SrtA plasmid (gift from Hidde Ploegh. Addgene plasmid #51141) was transformed into competent BL21 E. coli and grew on an LB-agar plate added with kanamycin (30μg/mL). Bacteria colonies were picked inoculated in 10mL of LB broth in the presence of kanamycin (30μg/mL). After overnight shaking (37°C, 220 rpm), the cultures were diluted 100-fold in kanamycin-LB media and shaken at 37°C until the optical density at 600 nm (OD 600) reached 0.4-0.6. SrtA expression was then induced via the addition of IPTG (400μM) and flasks were shaken for 3 hours at 37°C. After induction, cells were pelleted via centrifugation at 8000rpm for 15 minutes. Pellets were stored at 80°C until lysis was performed. Cells were lysed via a 30-minute incubation at 4°C while suspended in a lysis buffer (20mM Tris, 50mM NaCl, 0.2mg/mL lysozyme, 1X Halt EDTA-free protease inhibitor cocktail, and DNase I). The lysed cell solution was sonicated for 2 cycles lasting 3 minutes with a 30% duty cycle, at 20% amplitude, and with a 3-minute cool-down period between cycles. The lysate was centrifuged at 10,000×g and 4°C for 20 minutes and the supernatant was recovered for further purification. SrtA was purified through the use of His60 Ni Superflow resin and columns per the manufacturers protocol. Purified SrtA was concentrated with Ultra-15 Centrifugal Filter Units (3kDa MWCO, Amicon) and desalted with Zeba Spin desalting columns (7kDa MWCO, Thermo Fisher Scientific). The enzyme was aliquoted in pH 7.4 PBS and stored at 80°C until use. The concentration of aliquoted SrtA was measured via an Ellmans assay to detect the single, free sulfhydryl of SrtA.

3.4 Hydrogel Photopolymerization for Characterizing Softening

For experiments related to characterizing SrtA-mediated softening, hydrogels were fabricated by reacting PEG8NB with bis-cysteine containing peptides (e.g., KC-LPRTG-CK, KC-LPRTA-CK) via thiol-norbornene photo-click chemistry. PEG8NB

and peptides were mixed at a stochiometric ratio of thiol to norbornene (thiol / norbornene = R) with photoinitiator LAP (1mM). The precursor solution was injected between two glass slides separated by 1mm Teflon spacers, and exposed to 365nm light (5mW/cm^2) for 2 minutes. Hydrogels were swollen in a pH 7.4 PBS solution overnight prior to softening experiments.

3.5   Hydrogel Photopolymerization for Characterizing Ligand Exchange

For experiments related to the characterization of SrtA-mediated ligand exchange, hydrogels were fabricated by reacting PEG8NB with DTT or PEG4SH crosslinker and cysteine-containing peptides (C-LPRTGRGDS or C-LPRTGYK) via thiol-norbornene photo-click chemistry for stiffness or ligand exchange quantification, respectively. PEG8NB, crosslinker, and peptides were mixed at a stochiometric ratio of thiol to norbornene with photoinitiator LAP (1mM). The precursor solution was injected between two glass slides separated by 1mm Teflon spacers, and exposed to 365nm light (5mW/cm^2) for 2 minutes. Hydrogels for characterizing changes in stiffness via ligand exchange (PEG8NB-DTT-CLPRTGRGDS) were swollen in a pH 7.4 PBS solution within a 48-well plate overnight prior to ligand exchange. Hydrogels used for quantifying ligand exchange (PEG8NB-PEG4SH-CLPRTGYK) were swollen in separate 1.5mL microcentrifuge tubes containing 500μL pH 7.4 PBS solutions overnight prior to ligand exchange.

3.6   Sortase A-Mediated Hydrogel Softening

Softening of PEG-peptide hydrogels was achieved via the incubation of swollen hydrogels in a solution containing specified concentrations of SrtA and oligoglycine substrate (GGGGC, glycinamide, etc.). Storage moduli of the gels were measured before, at specified time points during, and after softening using oscillatory rheometry in strain sweep mode (8mm parallel plate geometry, 0.1% to 5% strain at 1Hz frequency, 750μM gap size).

3.7 Estimation of SrtA Diffusivity Within Softening Hydrogels

To determine the diffusivity of SrtA within a softening hydrogel, the mesh size of 4% weight PEG-KCLPRTACK hydrogels was measured at varied R ratios (R=1, 0.8, 0.6, and 0.4). Two sets of gels were formed as described above for each R ratio. The storage moduli of the first set of gels were obtained via oscillatory rheometry in strain sweep mode (8mm parallel plate geometry, 0.1% to 5% strain at 1Hz frequency) after an overnight swelling period. The second set of gels were immediately placed in a desiccator overnight, and the initial dry weight was measured the next day on a scale ($W_{Dry,1}$). The dry gels were then placed in ddH2O to swell overnight. The swollen mass was then measured via a scale ($W_{Swollen}$) and placed into a desiccator overnight to dry again. The final dry weight of the gels was then measured via a scale ($W_{Dry,2}$). The mass swelling ratio (Q_m) is calculated as $Q_m = \frac{W_{Swollen}}{W_{Dry,2}}$. Using the mass swelling ratio and the densities of the polymer (ρ_2=1.087g/mL for PEG) and of the solvent (ρ_1=1.00g/mL for water), the volumetric swelling ratio (Q_v) and polymer volume fraction (ν_2) could be calculated as:

$$Q_v = 1 + \frac{\rho_2}{\rho_1}(Q_m - 1) = \frac{1}{\nu_2} \tag{3.1}$$

We can calculate the average molecular weight between crosslinks via the use of the equation below. In this equation, $\bar{\nu}$ is the specific volume of the polymer ($\bar{\nu} = \frac{1}{\rho_2}$=0.92 ml/g for PEG), ν_1 is the molar volume of the solvent (18cm^3/mol for water), $X_{1,2}$ is the polymer-water interaction coefficient (0.45 for PEG), and $\overline{M}_n$ represents the molecular weight of the polymer (20000g/mol for the PEG used).

$$\frac{1}{\overline{M}_c} = \frac{2}{\overline{M}_n} - \frac{\frac{\bar{\nu}}{\nu_1}(ln(1-\nu_2) + \nu_2 + X_{1,2}\nu_2^2)}{\nu_2^{\frac{1}{3}} - \frac{\nu_2}{2}} \tag{3.2}$$

The root-mean-squared end-to-end distance between two crosslinks ($(\overline{r_0^2})^{\frac{1}{2}}$) can be calculated as the following, in which l is the average bond length of the polymer backbone, C_n is the Flory characteristic ratio (6.9 for PEG), n is the number of bonds

within the repeat unit of the polymer (3 for PEG), and M_r is the molecular weight for the polymer repeat unit (44g/mol for PEG):

$$(\overline{r_0^2})^{\frac{1}{2}} = l(C_n \frac{n\overline{M}_c}{M_r})^{\frac{1}{2}} \tag{3.3}$$

Finally, the mesh size can be calculated using the following equation:

$$\xi = \nu_2^{-\frac{1}{3}} (\overline{r_0^2})^{\frac{1}{2}} \tag{3.4}$$

The diffusivity of SrtA in the hydrogel was then predicted via the use of a model adapted by Lustig and Peppas [55]:

$$\frac{D}{D_0} = e^{-\frac{\gamma}{Q_v - 1}} (1 - \frac{r_s}{\xi}) \tag{3.5}$$

In which γ, the ratio of critical volume required for movement of diffusant over the average free volume per solvent molecule, is assumed 1, and r_s is the hydrodynamic radius of the SrtA heptamutant. To estimate the hydrodynamic radius of heptamutant SrtA, the protein structure was predicted via the use of I-TASSER suite [56]. The hydrodynamic radius and diffusivity were obtained via the use of HydroPRO (r_s=1.592nm, D_0=1.01$\times 10^{-10}$ m^2/sec).

3.8   Sortase A-Mediated Ligand Exchange and Characterization

Ligand exchange in PEG8NB-KCLPRTACK-CLPRTGRGDS hydrogels was achieved by incubating the swollen gels in a buffered solution containing 25μM SrtA and 12mM GGGGC for 4-hours. Gels were subsequently washed overnight with PBS prior to measurement. The storage moduli of the gels were measured before and after treatment using oscillatory rheometry in strain sweep mode (8mm parallel plate geometry, 0.1% to 5% strain at 1Hz frequency). Gels were treated with Ellmans reagent to qualitatively confirm GGGGC immobilization.

Quantification of ligand exchange in PEGNB-PEGSH-CLPRTGYK hydrogels was achieved by incubating swollen gels in a 500μL buffered solution containing specified

concentrations of SrtA and 24mM glycinamide for specified treatment times within 1.5mL microcentrifuge tubes. The PBS solutions used for swelling were collected and saved for determining immobilization efficiency. Treatment solutions were collected for release quantification after the specified treatment times. Quantification of immobilization efficiency was achieved via use of MBTH and Tyrosinase to determine free CLPRTGYK which was not immobilized within the PEGNB network. Release was quantified via the use of MBTH and Tyrosinase to determine the concentration of cleaved GYK within the treatment solution and normalized with respect to immobilized CLPRTGYK determined with respect to each gel.

In brief, a 5mM stock solution of MBTH was prepared in pH 6.0 PBS, a 1kU/mL Tyrosinase stock solution was prepared in pH 7.4 PBS, and a 1mM tyramine solution was prepared in pH 7.4 PBS. Six serial 2-fold dilutions of the tyramine standards were created with a PBS blank. 20μL of each standard and unknown (PBS wash solutions and release treatment solutions) was added to a 96-well plate (in triplicate). 40μL of the 5mM MBTH solution was added to each well, followed by 100μL of pH 7.4 PBS, and then 40μL of 1kU/mL Tyrosinase. The solutions were allowed to react for 30 minutes at room temperature while covered. The absorbance at 460nm of each well was measured, and the concentration of tyrosine within each swelling and treatment solution was calculated based on the tyramine standard.

3.9   Cell Culture

Human mesenchymal stem cells were maintained in low glucose Dulbeccos Modified Eagles Medium (DMEM) supplemented with 10% fetal bovine serum (FBS), 1ng/mL basic fibroblast growth factor (bFGF), and 1X penicillin streptomycin. bFGF was supplemented in the media at 1ng/mL as this concentration has been shown to maintain viability and proliferation of hMSCs during in vitro culture [57]. Media was refreshed every 23 days.

Fibroblast (NIH 3T3) cells were maintained in high glucose Dulbeccos Modified Eagles Medium (DMEM) supplemented with 10% fetal bovine serum (FBS) and 1X penicillin streptomycin. Media was refreshed every 23days.

3.10   hMSC Encapsulation

Prior to encapsulation, hMSCs were trypsinized, counted via a hemocytometer, and resuspended in Dulbeccos phosphate buffered saline (DPBS). Resuspended cells were introduced into a pre-mixed precursor solution (5×10^6 cells/mL) containing 3.5% PEG8NB, 1mM CRGDS, 50% KCGPQGIWGQCK (MMP), and 50% KCL-PRT(A/G)CK (inert/softenable, respectively) (R=1). Precursors were sterile-filtered prior to addition. Photoinitiator LAP was added at 1mM and the solution mixed. The cell-precursor solutions were pipetted into modified 1mL syringe molds and exposed to UV-light (365nm, 5mW/cm^2) for 2 minutes. Gels were transferred to a 24-well plate containing fresh media.

3.11   Softening of hMSC-Laden Hydrogels

Following encapsulation, hMSC-laden hydrogels were cultured in media for 7 days prior to SrtA-induced softening. Media was refreshed every 23 days. Softening was achieved through incubation of hydrogels with media containing 25μM SrtA and 12mM glycinamide for 4 hours on day 7 post-encapsulation. Gels were subsequently washed with fresh media for 4 hours to remove remaining SrtA and glycinamide and media refreshed. Media was refreshed every 2-3 days. Live/dead staining and confocal microscopy imaging (Olympus Fluoview FV100 laser scanning microscope) were performed on days 1, 7, and 14 post-encapsulation to assess cell viability and morphology. At least three z-stacked images per gel (10 slices, 100μm overall thickness) were taken. F-actin and DAPI stain imaging were performed on day 14 post-encapsulation for assessing cytoskeletal structure and cell morphology. Circularity and average cell area values were measured using ImageJ software from the F-actin/DAPI stained

confocal images Circularity and average cell area values were measured using ImageJ software from the F-actin/DAPI stained confocal images. Circularity is quantified as $4\pi\frac{\text{Area}}{\text{Perimeter}^2}$ and the area was quantified using the Analyze Particles function in ImageJ.

3.12 Removal of Pendant Cell-Adhesion Peptide in 2D Fibroblast Culture

1 day prior to 3T3 fibroblasts cell seeding, 4% wt PEG8NB-1mM CLPRTGRGDS-PEG4SH gels were formed within a 15-well angiogenesis plate (15-μslide IbiTreat, IBIDI). Precursor solutions were sterile filtered prior to usage. Precursors were mixed with 1mM LAP, injected into wells, and subjected to UV-light (365nm, 5mW/cm^2) for 2 minutes. Wells were filled with 50μL of media to allow for hydrogel swelling overnight. After swelling and prior to cell seeding, the fibroblast cells were trypsinized, counted (Countess$^{©}$ II Automated Cell Counter, ThermoFisher), and resuspended in media at 10^6 cells/mL. Swelling media was removed from the angiogenesis plate and replaced with 50μL of the cell suspension per well (5$\times$10^4 cells/well seeding). Cells were given one day to grow prior to treatment. The next day, the media was removed and replaced with corresponding treatment media (conditions: normal media, 6mM glycinamide only, 25μM SrtA only, and 25μM SrtA with 6mM glycinamide). Cells were continuously imaged via 4X brightfield montage and z-stack images (Lionheart FX automated microscope, BioTek) for 48 hours with 2-hour imaging intervals. Treatment media was refreshed every 24 hours. Images were analyzed in ImageJ for morphological quantification of cell cluster area and aspect ratio.

3.13 Fibroblast Encapsulation

Prior to encapsulation, 3T3 fibroblasts were trypsinized, counted (Countess$^{©}$ II Automated Cell Counter, ThermoFisher), and resuspended in DPBS. Resuspended cells were introduced into a pre-mixed precursor solution (5$\times$10^6 cells/mL) containing

2% wt PEG8NB, 1mM CLPRTGRGDS, and KCGPQGIWGQCK (R=1). Precursors were sterile-filtered prior to addition. Photoinitiator LAP was added at 1mM and the solution mixed. The cell-precursor solutions were pipetted into modified 1mL syringe molds and exposed to UV-light (365nm, 5mW/cm^2) for 2 minutes. Gels were then transferred to a 24-well plate containing fresh media.

3.14 Removal of Pendant Cell-Adhesion Peptide in 3D Fibroblast Culture

After encapsulation, treatment gels were incubated in media containing 25μM SrtA and 6mM glycinamide for 24 hours. Non-treated gels were incubated in fresh media. The treatment media was replaced with fresh media for 4 hours to wash the gels, and subsequently cultured within fresh media for the remainder of the study. Media was refreshed every 2-3 days. Live/dead staining and confocal microscopy imaging (Olympus Fluoview FV100 laser scanning microscope) were performed on days 1, 7, and 14 post-encapsulation to assess cell viability and morphology. At least three z-stacked images per gel (10 slices, 100μm overall thickness) were taken. F-actin and DAPI stain imaging were performed on day 14 post-encapsulation for assessing cytoskeletal structure and cell morphology.

3.15 Statistical Analysis

A two-way analysis of variance (ANOVA) was performed with Tukeys multiple comparison test to evaluate significance of softening of gels with varied PEG macromer concentration and "A" and "G" content. For hMSC area and circularity analysis, two-tailed t-tests were performed with Welchs correction for differences in sample sizes. For the analysis of GYK ligand removal, a one-way ANOVA was performed with Tukeys multiple comparison test. Single, double, triple, and quadruple asterisks represent p<0.05, 0.01, 0.001, 0.0001, respectively. All experiments were completed independently three times. Quantitative results are presented as mean $\pm$ SEM.

CHAPTER 4. RESULTS AND DISCUSSION

4.1 The Role of Material Selection in 3D Cell Culture

Throughout this work, hydrogel formation was performed through the use of the cytocompatible photo-click thiol-norbornene chemistry. A basic schematic of the chemistry is shown in Figure 4.1 below. This chemistry has been previously shown to be cytocompatible for the formation of cell-laden hydrogels [58, 59].
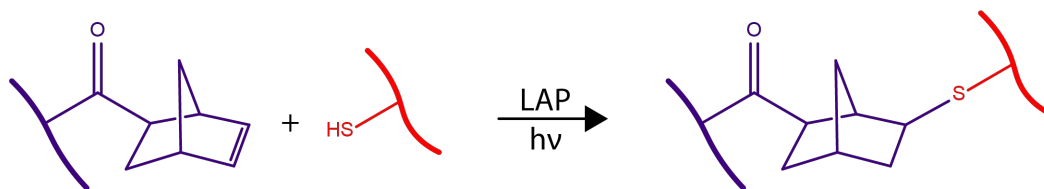
Fig. 4.1: A schematic of the photo-click thiol-norbornene light-initiated chemistry.

The selection of specific materials for use in 3D and 4D cell culture can have a significant impact on cell fate processes. For example, preliminary studies of this thesis project were focused on using synthetic or natural materials for encapsulation of human induced pluripotent stem cell (hiPSC). Synthetic hydrogels were crosslinked from 8-arm PEGNB macromer and protease-sensitive bis-cysteine crosslinker (KCGPQG ↓ IWGQCK), as well as pendant cell adhesion peptide (CRGDS). On the other hand, natural material-based hydrogels were prepared using gelatin-norbornene (GelNB), which was crosslinked with PEG4SH. Dispersed hiPSCs were encapsulated in either natural or synthetic-based hydrogels and cultured for 4 days. While hiPSCs formed spheroids in both PEG- and gelatin-based hydrogels, cell clusters in PEG-based hydrogels were more irregular than those in the gelatin-based hydrogels (Figure 4.2).

The irregular cell cluster morphology observed in the PEG-based hydrogels were potentially a result of cell-mediated attachment and remodeling/cleavage of the matrix. On the other hand, the complex composition of gelatin within the natural-based hydrogels likely contains other motifs that affected the morphogenesis of the encapsulated hiPSCs. Future studies are required to elucidate the underlying mechanism leading to confined spreading of hiPSCs in gelatin-based hydrogels. Nonetheless, this preliminary study has demonstrated the cytocompatibility of thiol-norbornene hydrogels for stem cell encapsulation.
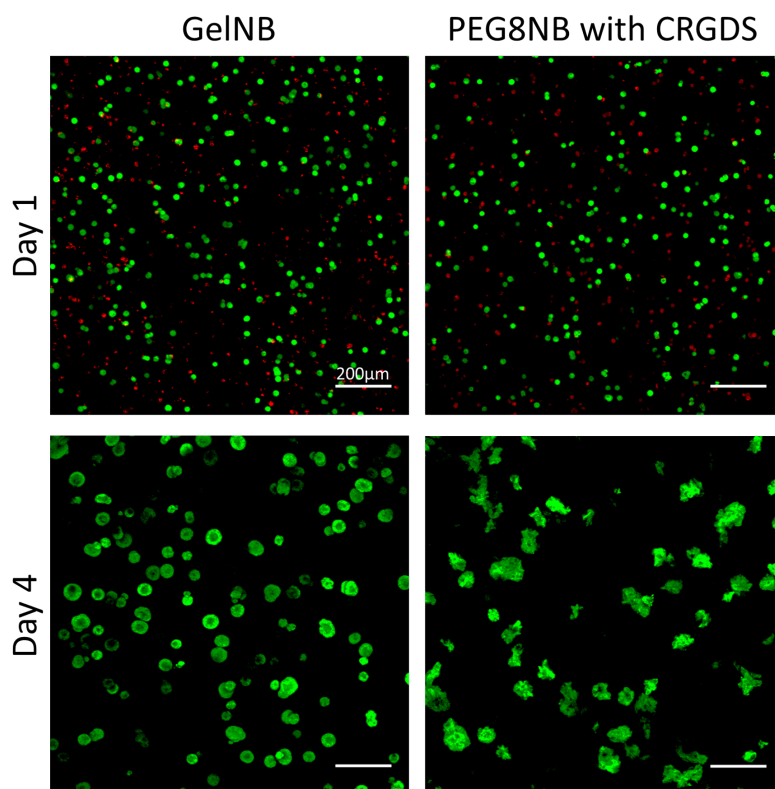
Fig. 4.2: Representative z-stack images (20 slices - 5μm each - 100μm total) of live and dead stained hiPSC (P3, 5$\times$10^6 cells/mL) imaged on days 1 and 4 post-encapsulation (scale bar=200μm). hiPSCs were encapsulated within either 2% wt GelNB-2%PEG4SH(GelNB) or 2.5% wt PEG8NB-4.5mM KCGPQG↓WGQCK-1mM CRGDS (PEG8NB) hydrogels. Gels were maintained in Essential 8 media with Essential 8 media supplement and 10μM ROCK inhibitor (Y-27632). (Unpublished Data).

4.2 SrtA Heptamutant Diffusivity Within Hydrogels of Varied Stiffness

Heptamutant SrtA was utilized throughout this work due to its mutations that afford an increased and calcium-independent reactivity [42]. Since SrtA needs to infiltrate in hydrogel to achieve softening, its diffusion in a highly swollen hydrogel was first approximated. The structure of SrtA was predicted via the I-TASSER suite [56] and is shown in Figure 4.3. This structure was introduced into HydroPRO to estimate the hydrodynamic radius and diffusivity of SrtA. The calculated hydrodynamic radius was estimated as 1.592nm and the corresponding diffusivity of SrtA in water was estimated to be 1.01×10^{-10} m^2/sec. Next, hydrogels were crosslinked with different thiol:norbornene ratio (R), which yielded different shear moduli (G). The moduli data were correlated with corresponding mesh size (calculated from hydrogel swelling ratios Figure 4.4a). This range of mesh sizes was then used to estimate the diffusivity of SrtA within these hydrogels according to the Lustig-Peppas approximation (Figure 4.4b) [55].
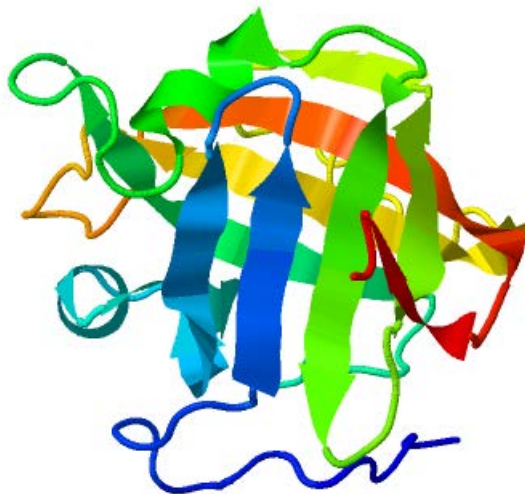
Fig. 4.3: Predicted structure of SrtA obtained via the use of I-TASSER suite.

a. Mesh size vs Modulus

b. Diffusivity vs Modulus
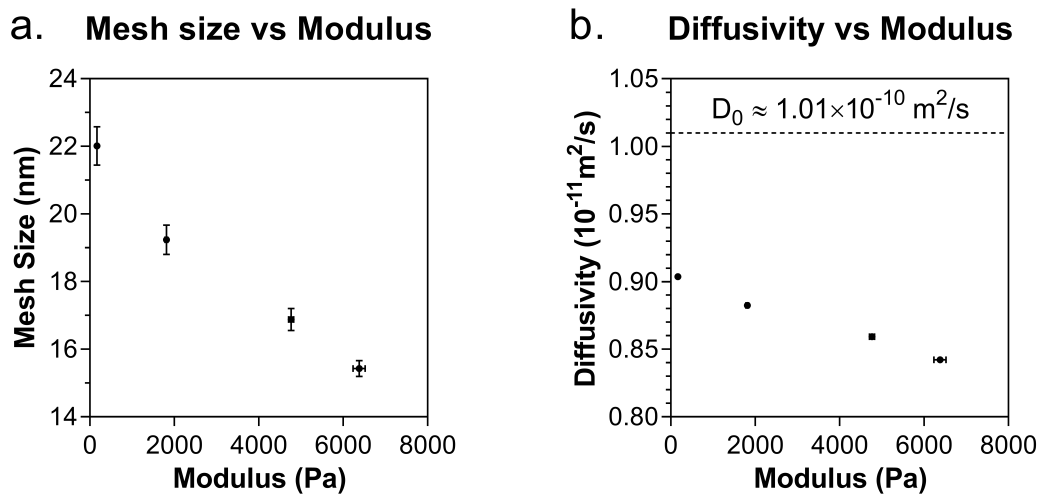
Fig. 4.4: (a) Mesh size measurements of hydrogels at varied stiffnesses. (4% wt PEG8NB-KCLPRTACK, R=1,0.8,0.6,0.4) (b) Estimated SrtA diffusivity within hydrogels at varied stiffnesses.

Based the relatively small difference in the estimated enzyme diffusivity (e.g., 0.84 to 0.90 $\times 10^{-10}$ m^2/s) in gels of varying stiffnesses, we reasoned that the process of softening would not drastically affect the diffusivity of SrtA within the hydrogel network. As the gels become softer, the enzyme would diffuse more readily through the matrix. It is important to note that the diffusion of SrtA would, however, be affected by binding with immobilized substrate (e.g., LPRTG) in the hydrogel network, which is not included in the estimation of SrtA diffusivity above.

4.3 Concept of SrtA-Mediated Softening of PEG-Peptide Hydrogels

SrtA has been widely used for a variety of bioconjugation applications, including protein tagging [45], peptide cyclization [46], and protein immobilization [60]. Recently, SrtA has been utilized in the formation of hydrogels and has allowed for reversibly stiffening and softening hydrogel networks cyclically [43, 50, 51]. We en-

visioned the utilization of SrtA as a means to provide precise control over hydrogel softening. This was achieved through forming hydrogels with the Leu-Pro- Arg-Thr-Gly SrtA linker. A peptide sequence not sensitive to SrtA (i.e. LPRTA) was used to provide tunable hydrogel softening. Hydrogels could be initially formed by a variety of crosslinking methods, given they do not interfere with sequence integrity. Formation of hydrogels within this work was achieve through cytocompatible and bio-orthogonal thiol-norbornene photo-click reaction of PEG8NB with bis-cysteine containing SrtA-sensitive (KCLPRT**G**CK, "G") or SrtA-insensitive (KCLPRT**A**CK, "A") peptide. Flanking lysine residues were included to improve their solubility. Upon incubation of these hydrogels within a solution containing SrtA and an oligoglycine substrate, SrtA-sensitive linkages (G) undergo transpeptidation leading to softening, while SrtA-insensitive linkages (A) would remain intact as illustrated in Figure 4.5.
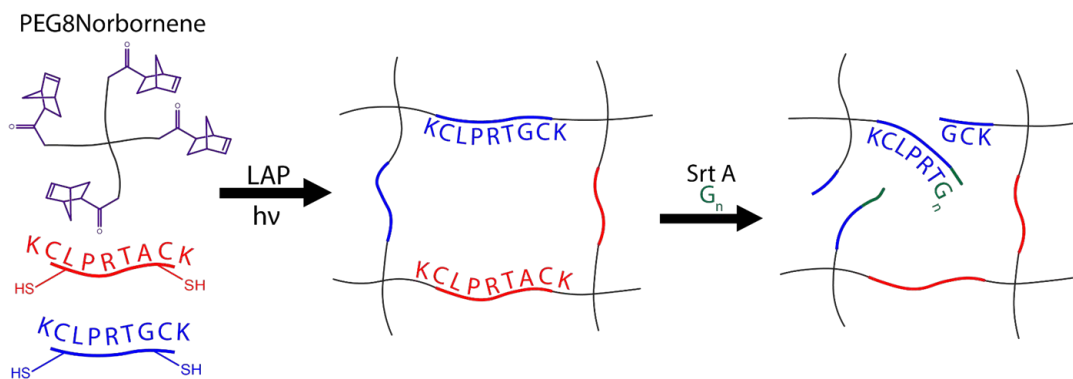

Fig. 4.5: Schematic of the on-demand SrtA-mediated softening system. Hydrogels are formed via photo-click thiol-norbornene chemistry and SrtA-sensitive crosslinks (KCLPRTGCK) are cleavable via the introduction of SrtA and an oligoglycine substrate (G_n). Inert crosslinks (KCLPRTACK) remain unaffected by the introduction of SrtA and G_n.

4.3.1 Characterizing SrtA-Mediated Softening

Utilizing the hydrogel network structure shown in Figure 4.5 (3 wt% PEG8NB, A:G ratio=50%:50%, and R=1, G_0~2100 Pa), we first sought to investigate the efficiency of SrtA-mediated softening at specific SrtA concentrations (Figure 4.6a). At lower concentration of SrtA (e.g., 10μM), the moduli of hydrogels decreased much slower than that with higher SrtA concentrations. Furthermore, a SrtA concentration of 25 or 50 μM yielded similar softening profiles, suggesting that the transpeptidation reaction occurred in the hydrogel was rapid and diffusion-limited.

The concentration of oligoglycine substrate was subsequently investigated. As shown in Figure 4.5b, a higher degree of softening was observed at increasing concentration of GGGGC (with 25μM SrtA, Figure 4.6b). This experiment was repeated with the use of glycinamide in place of GGGGC and a similar trend was observed (data not shown). In the absence of an oligoglycine substrate, the SrtA reaction undergoes a much slower irreversible hydrolysis reaction, which converts LPRTG into LPRT-OH with the release of the glycine [40]. This hydrolysis reaction is always in competition with the natural transpeptidation reaction, but as seen in the figure it is noticeable slower (25% softening after 24 hours). When limiting the available time for transpeptidation to occur, by transferring the hydrogel to fresh media which does not contain SrtA or oligoglycine substrate, we were able to stop the softening process from completing (Figure 4.6c). The final moduli of these gels (at ~0.5, 2.5, and 4 hours) were constant at around the same level as when they were first transferred to enzyme-free solutions.

We also investigated the use of different oligoglycine substrates for softening our hydrogel network (12mM Glycinamide vs 12mM GGGGC) and saw little difference in degree of softening achieved (3% PEG, A:G ratio=50%:50%, R=1, 25μM SrtA) (Figure 4.6d). This result demonstrated the applicability of different oligoglycine substrates for producing similar softening effects.
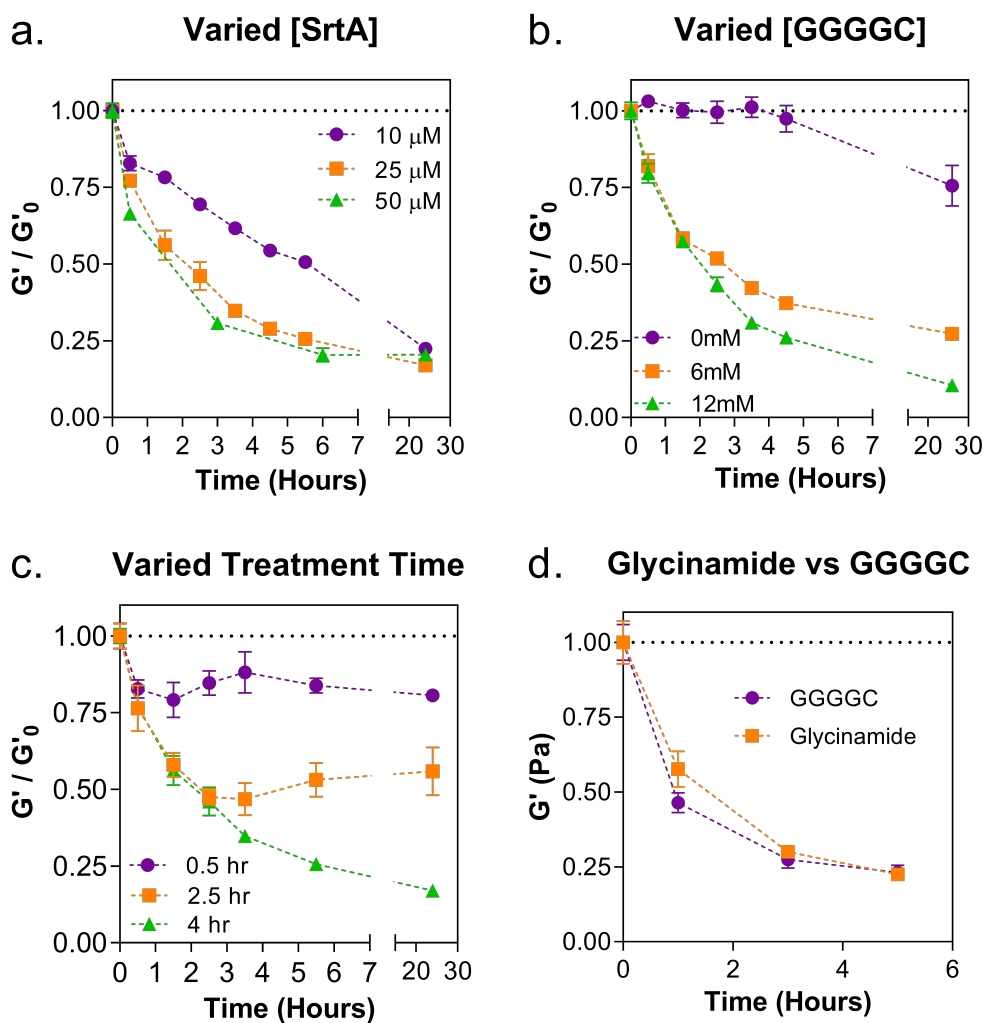
Fig. 4.6: Characterization of various parameters in the SrtA-mediated softening system (3% wt PEG8NB, R=1, 50% A: 50% G) on hydrogel moduli measured via shear-rheology at various time points before, during, and after treatment. (a) The effect of SrtA concentration on the stiffness of gels also incubated with 12mM GGGGC. (b) The effect of GGGGC concentration on the stiffness of gels also incubated with 25μM SrtA. (c) The effects of treatment time on the stiffness of gels treated with 25μM SrtA and 12mM GGGGC (0.5, 2.5, and 4.0 hour treatment). (d) Utilization of different oligoglycine (Glycinamide and GGGGC) substrates in the softening of hydrogels. (n=3).

In an attempt to explore the reversibility of network softening, a new peptide sequence (i.e., KCLPRTGGGCK) was used to crosslink hydrogel. This peptide was used because after SrtA-mediated transpeptidation the linker was cleaved into KCL-PRTG and GGGCK motifs, which were both still linked to the hydrogel network. Ideally, these two pendant peptides could be ligated by additional SrtA, leading to hydrogel stiffening. Experimentally, reversible hydrogel softening/stiffening was explored using gels formed from PEG8NB with 50% DTT crosslinker and 50% KCL-PRTGGGCK peptide linker. Control gels not sensitive to SrtA treatment were created with PEG8NB and 100% DTT crosslinker. Initial softening was performed through treatment with 25μM SrtA and 12mM glycinamide. Gels were washed of unreacted glycinamide and subsequently incubated with 25μM SrtA for 4 hours to initiate re-stiffening. Unfortunately, limited re-stiffening was achieved (Figure 4.7). This may be because the cleaved pendant GGG peptide became inaccessible to the LPRT-SrtA complex. As the linkages are cleaved, the gels swell more leading to an increase in the distance between pendant LPRTG and pendant GGG.
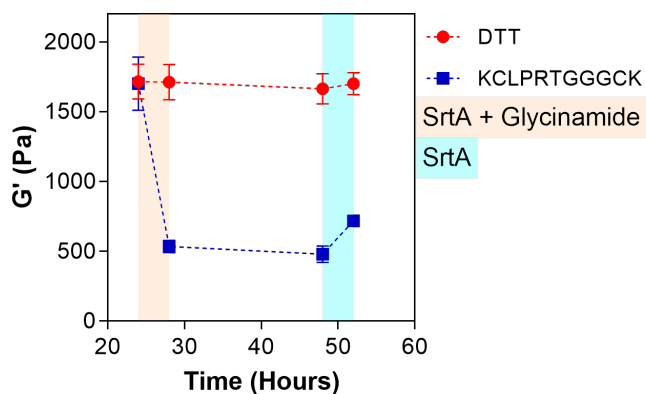
Fig. 4.7: Attempted re-stiffening of SrtA-sensitive hydrogels. Hydrogels were formed with PEG8NB and either 100% DTT or 50% KCLPRTGGGCK with 50% DTT. Gels were swollen overnight prior to treatment for 4 hours with 25μM SrtA and 12mM glycinamide. Gels were subsequently washed and treated for 4 hours with 25μM SrtA.

4.3.2 Tuning SrtA-Mediated Softening via Hydrogel Composition

By adjusting the initial PEG8NB macromer concentration we were able to produce gels with varied initial moduli, each of which is significantly softened when treated with SrtA and an oligoglycine substrate (A:G ratio=50%:50%, R=1, 25μM SrtA, 12mM GGGGC. Figure 4.8a). To account for increasing SrtA-sensitive ligand concentration, it may be necessary to adjust treatment time as the overall ligand concentration would vary at similar A:G ratios.

The final moduli of the fully softened hydrogels with the same PEG8NB macromer content (3 wt%) were easily tuned by adjusting the ratio of A and G (Figure 4.8b). In addition, by adjusting concentrations of PEG8NB macromer and the A:G ratio, we were able to form gels with different initial moduli but were softened to the same final moduli after 4 hours of SrtA treatment. Even further we were able to create gels with similar initial moduli but were softened to different final moduli after SrtA treatment (25μM SrtA and 12mM GGGGC. Figure 4.8c). Together, these results demonstrated that the hydrogels can be controllably tuned to specific moduli by adjusting macromer compositions or by adjusting the enzyme treatment conditions.
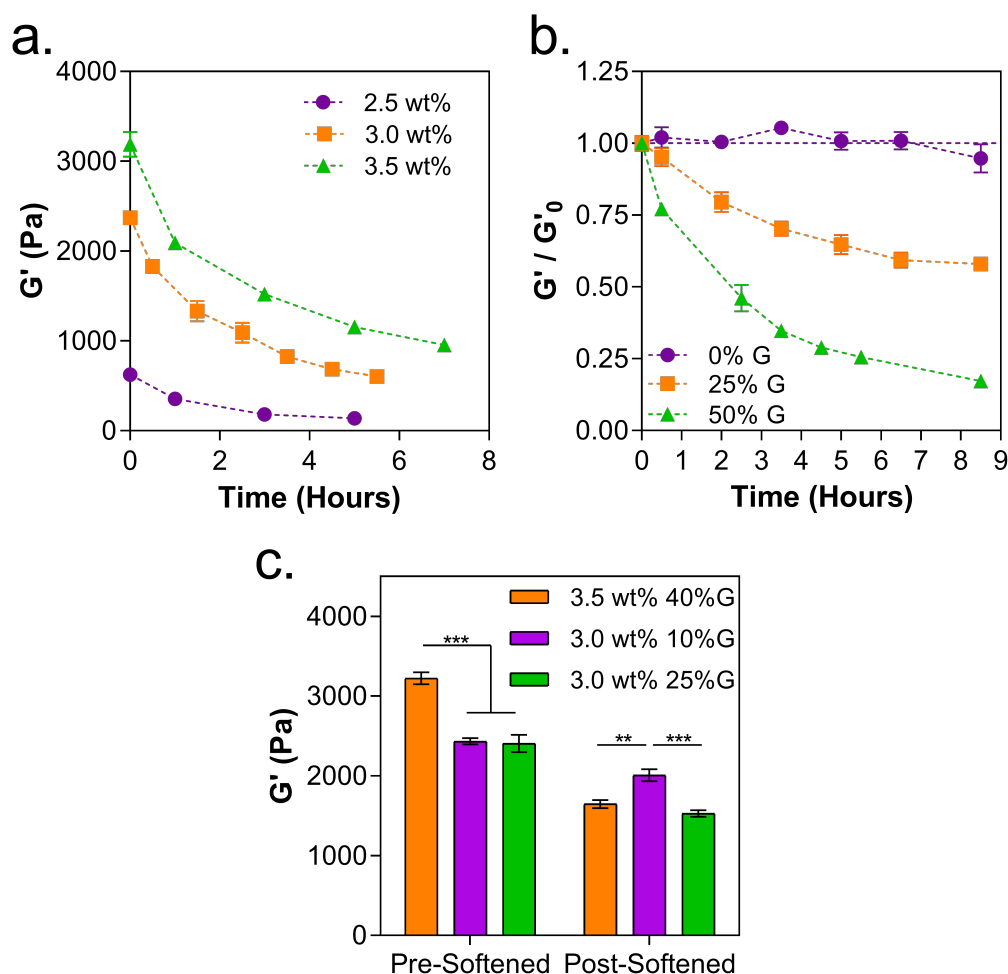
Fig. 4.8: Controlling the initial and final moduli of SrtA-softenable hydrogels via PEG macromer concentration and degradable composition (treated with 25μM SrtA and 12mM GGGGC). (a) Initial and final hydrogel moduli tuned via PEG8NB macromer concentration (50% A:50% G, R=1). (b) Tunable softening of 3% wt PEG8NB hydrogels with varied A and G compositions. The remainder of the gel crosslinks were A linkages (i.e. 50% G and 50% A). (c) Softening of tuned hydrogels via PEG macromer concentration and A:G composition to similar levels after a 4-hour treatment period. (n=3).

4.3.3   Effect of SrtA-Mediated Softening on hMSC Morphology

The SrtA-mediated softening hydrogel was used as a means to study the effects of temporally softening the matrix on morphology of hMSCs. Hydrogels have been used extensively for 3D culture of hMSCs. Studies have reported that hMSCs respond to varying stiffnesses by elongating in softer environments and remaining spherical in stiffer environments [4, 7]. To investigate the effects of SrtA-mediated softening on hMSCs, we encapsulated cells within PEGNB hydrogels of which 50% of crosslinks contained either SrtA-sensitive G or insensitive A peptide crosslinker, while the remaining 50% of crosslinks were composed of MMP-degradable crosslinker (e.g., KCGPQG↓IWGQCK). The inclusion of MMP-sensitive peptide allows for cells to remodel their local environment through secretion of proteases. The gels were also immobilized with 1 mM of a cell adhesion sequence RGDS to allow for cell attachment within the network. To induce matrix softening, gels were treated with 25μM SrtA and 12mM Glycinamide. Not surprisingly, gels crosslinked with SrtA-sensitive G peptide led to higher degree of hMSC spreading (Figure 4.9a). Image analysis results show that the cells cultured in the softened hydrogels were significantly more elongated and less circular (quantified as $4\pi\frac{\text{Area}}{\text{Perimeter}^2}$), Figure 4.9b). Cells in the softened hydrogels also spread more as quantified by the average area per cell (Figure 4.9c). Collectively, these results have demonstrated the applicability of the SrtA-mediated transpeptidation as an on-demand, tunable, and cytocompatible method for softening cell-laden hydrogels.
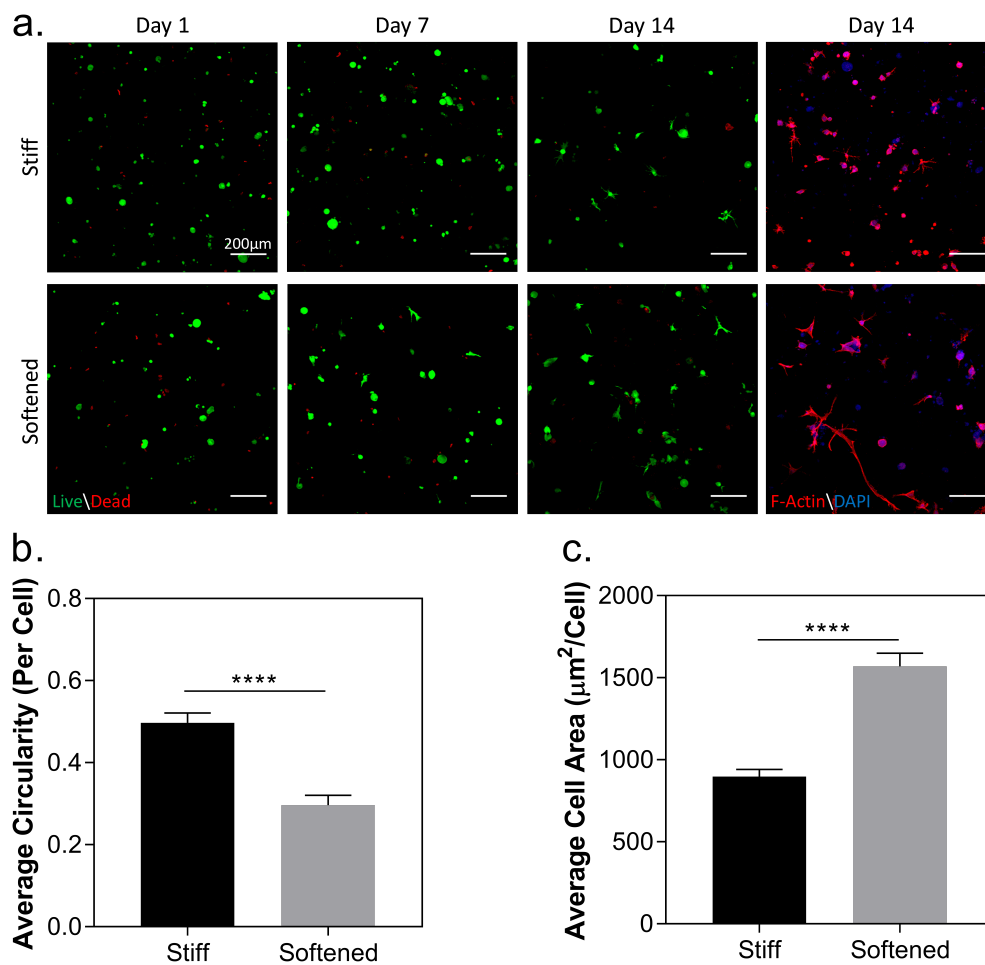
Fig. 4.9: Effect of SrtA-mediated softening on hMSC morphology. (a) Representative z-stack images of live and dead stained hMSCs (on days 1,7 and 14) and F-actin/DAPI staining (on day 14) encapsulated within 3.5% wt PEG-50% MMP-50% KCLPRT(A/G)CK-1mM CRGDS (R=1) hydrogels treated with 25μM SrtA and 12mM glycinamide for 4 hours on day 7. (b) Circularity and (c) average cell area of encapsulated hMSCs quantified in ImageJ from day 14 F-actin/DAPI staining. (n=85 cells for the stiff condition, n=142 cells for the softened condition).

4.4 SrtA-Mediated Ligand Exchange

In addition to controlled softening of cell-laden hydrogels, SrtA-mediated transpeptidation was also explored for dynamically introducing and removing bioactive motifs on demand. To achieve this, hydrogels were polymerized using thiol-norbornene photoclick chemistry. Pendant peptide ligands were immobilization into the network during gel crosslinking. To render the pendant ligand sensitive to SrtA-mediated transpeptidation, the sequence LPRTG was inserted before the actual bioactive motif. Through incubation with SrtA and an N-terminal glycine containing substrate (e.g., GGGRGDS, Glycinamide, etc.), the initially immobilized ligand can be removed or exchanged with another desired bioactive group (Figure 4.10).

Fig. 4.10: Schematic of SrtA-mediated ligand exchange system. Crosslinking and immobilization of pendant ligand initiated by photoinitiator LAP and UV (365nm) light exposure. Introduction of specific ligands into the system is achieved through treatment with the N-terminal Glycine containing ligand and SrtA. Exchange/removal of said ligand can be achieved through treatment with another oligoglycine substrate and SrtA.

4.4.1   Effects of Ligand Exchange on Hydrogel Stiffness

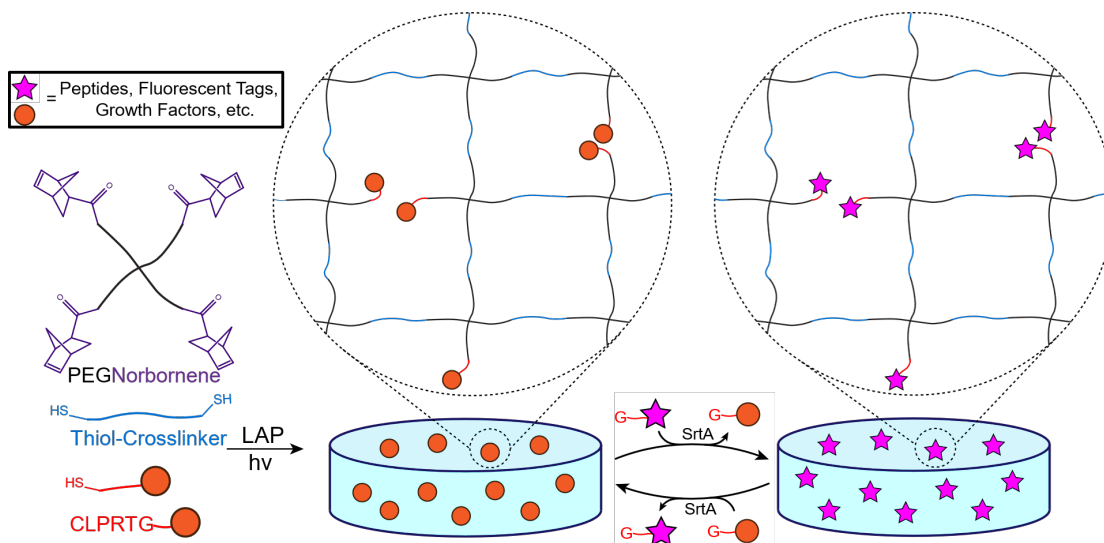We first sought to understand the effects of dynamic ligand exchange on the mechanical properties of the treated hydrogels. SrtA-sensitive pendant ligands (i.e., 0, 1, or 2 mM CLPRTGRGDS) were immobilized into hydrogels crosslinked by PEG8NB macromer and DTT crosslinker. Hydrogels immobilized with different concentrations of the peptide ligand did not yield significantly different initial moduli (Figure 4.11a). This makes sense, as the pendant ligand did not contribute to crosslinking density of the network. After treating the peptide-immobilized hydrogels with 25μM SrtA and 12mM GGGGC for 4 hours, moduli of hydrogels were measured again and no significant difference was found (Figure 4.11a), suggesting that the removal of pendant peptide ligands can be achieved independent of network crosslinking density. To confirm that GRGDS was displaced by GGGGC, the treated hydrogels were first washed to remove residual SrtA (which contains a single reactive cysteine residue) and any soluble unreacted GGGGC. The washed gels were then placed in a solution containing excess Ellmans reagent to label free cysteine residues that were immobilized within the hydrogel network after the SrtA-mediated ligand exchange. Gels which were formed with SrtA sensitive pendant groups (i.e., 1 mM or 2 mM CLPRTGRGDS) produced significant yellow tints after SrtA and GGGGC treatment associated with reacted Ellmans reagent compared to gels which had no SrtA-sensitive pendant groups (Figure 4.11b).
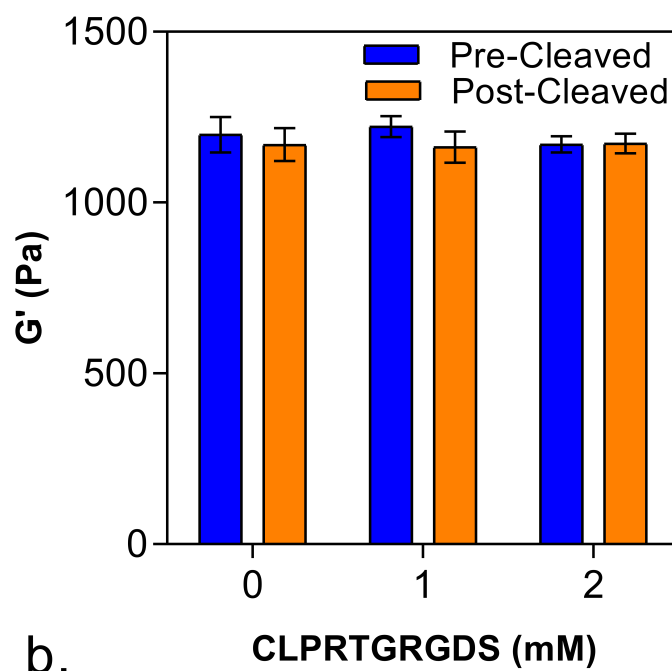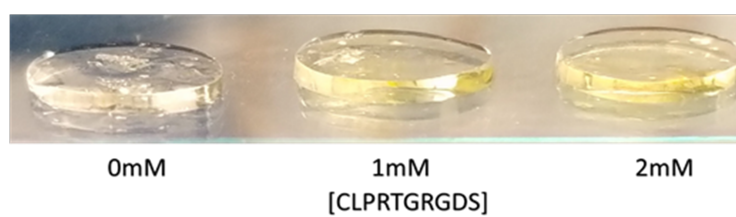
Fig. 4.11: (a) 3% wt PEG8NB-5mMKCLPRTACK-Varied CLPRTGRGDS (25μM SrtA, 12mM GGGGC, 4-hour treatment time). (b) Gels treated with Ellmans Reagent.

4.4.2   Quantification of Ligand Exchange

The efficiency of peptide ligand exchange was evaluated next using different SrtA concentrations. For this purpose, PEG8NB hydrogels were created with PEG4SH crosslinker and a SrtA-sensitive pendant peptide (CLPRTGYK). The removal of GYK from the immobilized CLPRTGYK was quantified by detecting the concentration of liberated tyrosine within solution using a modified MBTH assay. Briefly, a small aliquot containing the released GYK peptide was mixed with excess MBTH and 1 kU/mL tyrosinase. Tyrosinase catalyzes the oxidation of tyrosine residues into dihydroxyphenylalanine (DOPA), which is further oxidized into DOPAquinone and react with MBTH to form an MBTH-Quinone adduct. The latter had a detectable absorbance at 460nm (Figure 4.12).
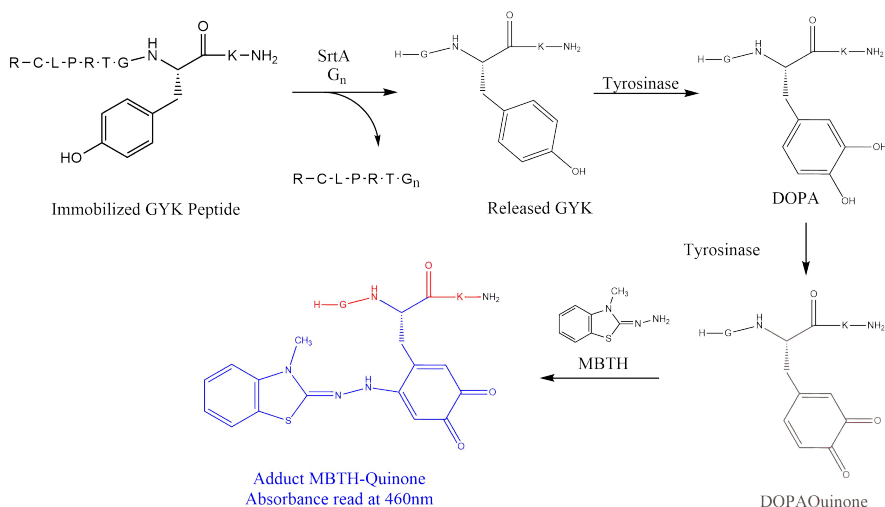
Fig. 4.12: Schematic for quantification of GYK removal via SrtA-mediated transpeptidation.

Experimentally, hydrogels were first washed to elute free CLPRTGYK that was not immobilized in the PEG-peptide hydrogel network. Next, this solution was collected to calculate the relative immobilization efficiency of the peptide within the hydrogels ($82.2\pm3.4\%$ immobilized) and for use in normalization of release data. After treatment of the gels for 4 hours with varied concentrations of SrtA and 24mM glycinamide (4-fold excess with respect to ligand concentration), the solutions were collected and soluble GYK measured to calculate percent released. We found that after 4 hours only 20% of GYK ligand was cleaved at 25μM SrtA. This is much lower than we would have expected based on softening completing after about 4 hours of treatment with 25μM SrtA. The high efficiency of softening is likely due to an increase in distance of the cleaved -LPRTG$_n$ and G- groups from each other within the softening network. If the oligoglycine substrate is not in close proximity to the thioester intermediate, it would be less likely to react with the intermediate. As the pendant ligand, GYK in this experiment, was cleaved from the network it remained in the solution and was free to diffuse throughout the matrix. It could react with the thioester intermediate, leading to the re-addition of the peptide. As the concentration of SrtA was increased, significantly more ligand was removed (Figure 4.13a). This was likely due to the increase in potential ligand exchange events as each SrtA enzyme can only interact with local pendants ligand groups. We next wanted to look at the possibility of extending treatment time as an alternative to using a higher concentration of SrtA. When the treatment time of gels was increased (25μM SrtA, 24mM glycinamide for 4, 8, or 24 hours), there was a significant and time-dependent increase in the total ligand removal (Figure 4.13b). Increasing enzyme incubation time would allow for the enzyme to interact with more pendant ligands within the gels. As the cytocompatibility of the SrtA transpeptidation was previously demonstrated in the softening of hMSC-laden hydrogels, the focus turned towards investigating SrtA-mediated ligand exchange within cell culture.
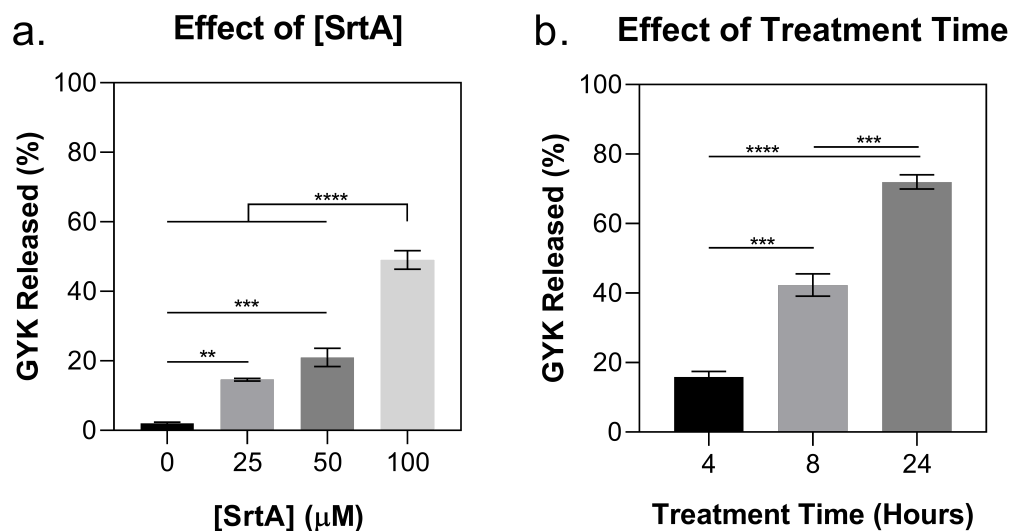
Fig. 4.13: Hydrogels were created with 4.5% wt PEG8NB-2.5mM PEG4SH-6mM CLPRTGYK. (a) Effect of SrtA concentration on ligand removal. Gels were treated with 24mM glycinamide and varied concentrations of SrtA for 4 hours. (b) Effect of treatment time with SrtA and glycinamide on ligand removal. Gels were treated with 24mM glycinamide and 25μM SrtA for varied treatment times. (n=3).

4.4.3 SrtA-Mediated RGDS Removal in 2D 3T3 Cell Culture

We next sought to test the ligand exchange system in cell culture. To do this we seeded 3T3 fibroblasts on top of hydrogels containing SrtA-sensitive RGDS pendant peptide (i.e., CLPRTGRGDS). The cells were allowed to grow for 1 day prior to treatment with one of the 4 conditions (i.e., normal media, glycinamide, SrtA, or SrtA and glycinamide). Live cell imaging was performed over 48 hours (with 2-hour intervals between images). From the brightfield images, it can be seen that cells spread less when treated with SrtA and glycinamide when compared to cell treated with one of the two or in control media (Figure 4.14a). This suggests that the integrin-ligand RGDS was removed from the hydrogel surface after SrtA treatment. Quantification results of average cell cluster area (Figure 4.14b) and average cell cluster aspect ratios (Figure 4.14c) using ImageJ software show the same trend. Cells treated with either glycinamide or SrtA alone also had a lower average cell cluster area and aspect ratio in comparison to the control group. As the SrtA reaction is able to facilitate hydrolysis, it is reasonable that some of the pendant RGDS motifs would be hydrolyzed over the 48 hours of SrtA incubation. Interestingly, the addition of glycinamide into the cell-culture media led to a yellow tinted solution. As the media contains phenol red, a pH indicator, this would signal that the glycinamide-media solution is not at physiological pH. This would likely affect natural cell processes such as spreading and survival. In comparison, these two conditions were more confluent and contained more spreading than the cells treated with SrtA and glycinamide together. This would support that the transpeptidation reaction led to increased RGDS removal in this condition.
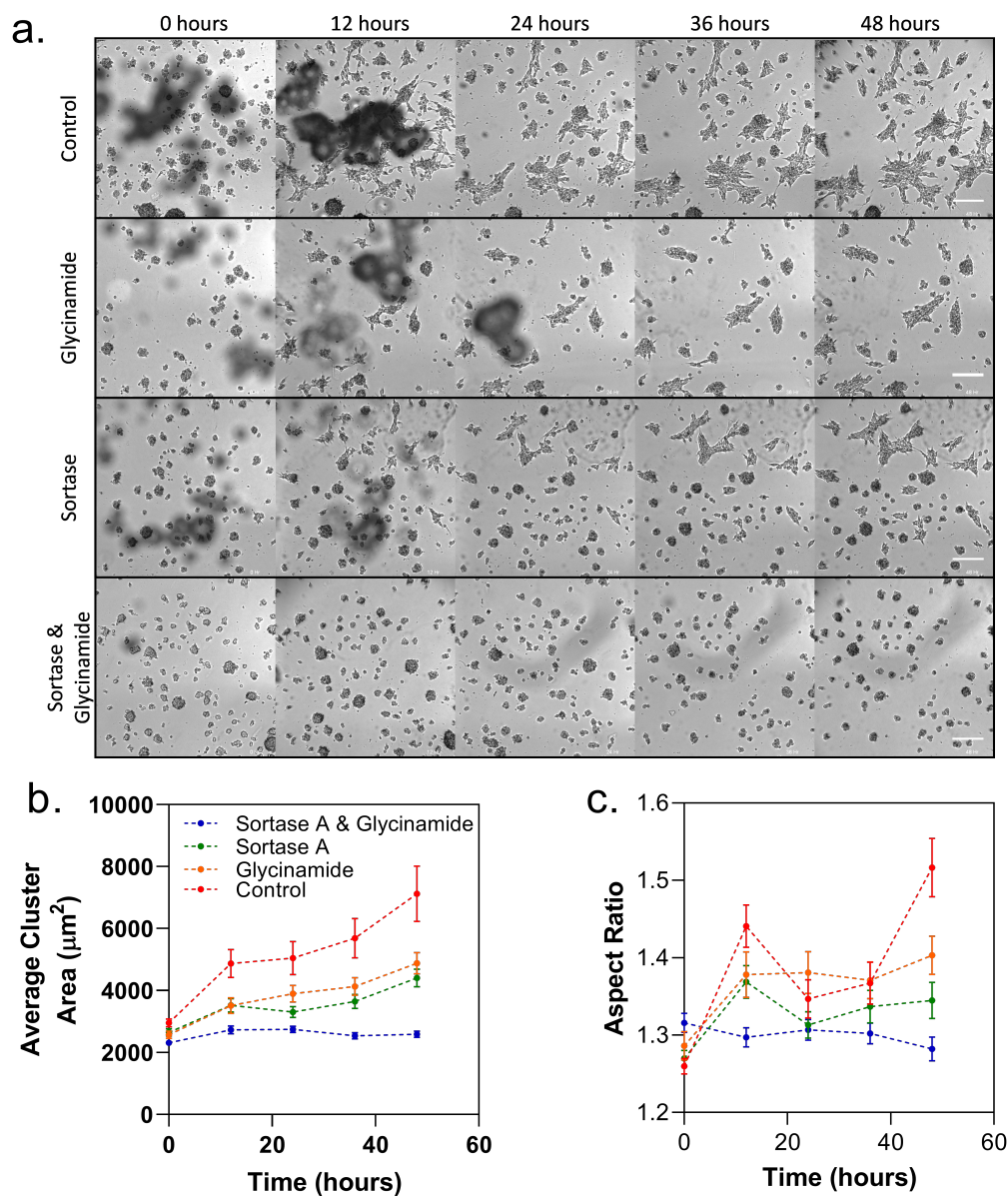
Fig. 4.14: SrtA-mediated removal of pendant RGDS motifs from 3T3 cells cultured on top of hydrogels. (a) Representative 12 hour brightfield images of 3T3 cells cultured on gels containing SrtA-sensitive RGDS peptide and treated with various conditions (scale bar = 200μm). (b) Quantification of average cell cluster area at 12-hour intervals from the four treatment conditions. (c) Quantification of average cell cluster aspect ratios at 12-hour intervals.

4.4.4   SrtA-Mediated RGDS Removal in 3D 3T3 Cell Culture

We next investigated whether the SrtA-mediated ligand exchange system could be used to affect adhesion of cells encapsulated within hydrogels. To achieve this, 3T3 fibroblasts were encapsulated in PEG-peptide hydrogels with immobilized SrtA-sensitive pendant RGDS ligand (i.e., CLPRTGRGDS). Gels were either treated with 25μM SrtA and 12mM glycinamide for 24 hours directly after encapsulation or were not treated. Cells encapsulated within gels that were treated with SrtA showed lower degree of spreading compared to their non-treated counterparts (Figure 4.15). These results suggested that SrtA-treatment led to removal of RGD ligands from the cell-laden hydrogels and in turn reduced spreading.
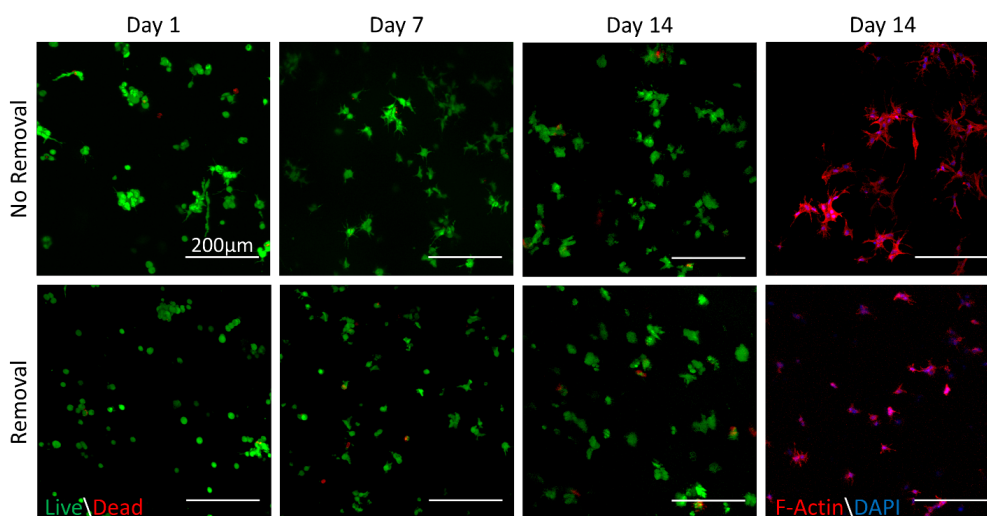
Fig. 4.15: Effect of SrtA-mediated GRGDS removal on 3T3 cell morphology. Representative z-stack images of live and dead stained (on days 1,7 and 14) and F-actin/DAPI stained (on day 14) 3T3 cells encapsulated within 2.5% wt PEG-MMP-1mM CLPRTGRGDS (R=1). Removal gels were treated with 25μM SrtA and 12mM glycinamide for 24 hours on day 0.

CHAPTER 5. SUMMARY AND RECOMMENDATIONS

5.1 Summary

In summary, a tunable hydrogel system capable of being softened enzymatically was developed. Softening was achieved using relatively low concentrations of SrtA. 4 hours of enzyme treatment was sufficient to reach a terminal degree of softening. Compared to non-dynamic hydrogels, hMSCs responded to softening of the matrix by spreading more. The use of SrtA as a means of introducing new ligands into the system was also investigated. Ligand removal from hydrogels treated with varied concentrations of SrtA and for varied treatment times was also characterized. Specifically, increasing the concentration of SrtA and treatment time both led to increased degrees of ligand exchange. In 2D culture, it was demonstrated that the removal of cell adhesion peptide (RGDS) via SrtA-mediated transpeptidation, decreased the spreading of 3T3 fibroblasts. On the other hand, a similar trend was observed for 3T3 fibroblasts encapsulated within hydrogels that were treated with SrtA to remove RGDS ligands. After RGDS removal, encapsulated cells exhibited less spreading when compared to the cells cultured within gels without RGDS removal.

5.2 Recommendations

Much of the work done in this thesis was focused on the use of inert PEG-based polymers with the inclusion of bioactive motifs (RGDS, GPQGIWGQ, etc.). Due to the specificity of SrtA transpeptidation, this softening and ligand exchange system can be adapted for use in natural material-based hydrogels such as gelatin and hyaluronic

acid. Natural materials are advantageous to synthetic polymers such as PEG, in that they often contain motifs for cellular adhesion and degradation, and they are derived from natural tissue. As the ligand exchange system has been characterized well outside of cell culture, further work into its utilization, such as demonstrating repeatedly exchanged motifs or growth factors may be desirable. As seen in wound healing, there is often dynamic changes in ECM proteins such as collagen. The reduction in collagen leads to a changes in local bioactive motifs and releases entrapped growth factors. To better recapitulate the dynamic environments seen naturally within the body, it is ideal to be able to mimic those changes in culture.

This work can also be furthered through the creation of a diffusion-kinetics model. A model would be applicable for predicting the completion of both the softening and ligand exchange systems. This would be useful for designing treatment conditions for future experiments.

LIST OF REFERENCES

LIST OF REFERENCES

[1] R. W. Tilghman, C. R. Cowan, J. D. Mih, Y. Koryakina, D. Gioeli, J. K. Slack-Davis, B. R. Blackman, D. J. Tschumperlin, and J. T. Parsons, "Matrix rigidity regulates cancer cell growth and cellular phenotype," *PLoS One*, vol. 5, no. 9, p. e12905, 2010. [Online]. Available: https://www.ncbi.nlm.nih.gov/pubmed/20886123

[2] F. Gattazzo, A. Urciuolo, and P. Bonaldo, "Extracellular matrix: a dynamic microenvironment for stem cell niche," *Biochim Biophys Acta*, vol. 1840, no. 8, pp. 2506–19, 2014. [Online]. Available: https://www.ncbi.nlm.nih.gov/pubmed/24418517

[3] M. Votteler, P. J. Kluger, H. Walles, and K. Schenke-Layland, "Stem cell microenvironments–unveiling the secret of how stem cell fate is defined," *Macromol Biosci*, vol. 10, no. 11, pp. 1302–15, 2010. [Online]. Available: https://www.ncbi.nlm.nih.gov/pubmed/20715131

[4] A. J. Engler, S. Sen, H. L. Sweeney, and D. E. Discher, "Matrix elasticity directs stem cell lineage specification," *Cell*, vol. 126, no. 4, pp. 677–89, 2006. [Online]. Available: https://www.ncbi.nlm.nih.gov/pubmed/16923388

[5] J. S. Park, J. S. Chu, A. D. Tsou, R. Diop, Z. Tang, A. Wang, and S. Li, "The effect of matrix stiffness on the differentiation of mesenchymal stem cells in response to tgf-beta," *Biomaterials*, vol. 32, no. 16, pp. 3921–30, 2011. [Online]. Available: https://www.ncbi.nlm.nih.gov/pubmed/21397942

[6] A. S. Rowlands, P. A. George, and J. J. Cooper-White, "Directing osteogenic and myogenic differentiation of mscs: interplay of stiffness and adhesive ligand presentation," *Am J Physiol Cell Physiol*, vol. 295, no. 4, pp. C1037–44, 2008. [Online]. Available: https://www.ncbi.nlm.nih.gov/pubmed/18753317

[7] S. R. Caliari, S. L. Vega, M. Kwon, E. M. Soulas, and J. A. Burdick, "Dimensionality and spreading influence msc yap/taz signaling in hydrogel environments," *Biomaterials*, vol. 103, pp. 314–323, 2016. [Online]. Available: https://www.ncbi.nlm.nih.gov/pubmed/27429252

[8] C. M. Madl, L. M. Katz, and S. C. Heilshorn, "Bio-orthogonally crosslinked, engineered protein hydrogels with tunable mechanics and biochemistry for cell encapsulation," *Adv Funct Mater*, vol. 26, no. 21, pp. 3612–3620, 2016. [Online]. Available: https://www.ncbi.nlm.nih.gov/pubmed/27642274

[9] P. J. Wipff, D. B. Rifkin, J. J. Meister, and B. Hinz, "Myofibroblast contraction activates latent tgf-beta1 from the extracellular matrix," *J Cell Biol*, vol. 179, no. 6, pp. 1311–23, 2007. [Online]. Available: https://www.ncbi.nlm.nih.gov/pubmed/18086923

[10] M. B. Serra, W. A. Barroso, N. N. da Silva, S. D. N. Silva, A. C. R. Borges, I. C. Abreu, and M. Borges, "From inflammation to current and alternative therapies involved in wound healing," *Int J Inflam*, vol. 2017, p. 3406215, 2017. [Online]. Available: https://www.ncbi.nlm.nih.gov/pubmed/28811953

[11] G. C. Gurtner, S. Werner, Y. Barrandon, and M. T. Longaker, "Wound repair and regeneration," *Nature*, vol. 453, no. 7193, pp. 314–21, 2008. [Online]. Available: https://www.ncbi.nlm.nih.gov/pubmed/18480812

[12] J. Rosinczuk, J. Taradaj, R. Dymarek, and M. Sopel, "Mechanoregulation of wound healing and skin homeostasis," *Biomed Res Int*, vol. 2016, p. 3943481, 2016. [Online]. Available: https://www.ncbi.nlm.nih.gov/pubmed/27413744

[13] S. Maxson, E. A. Lopez, D. Yoo, A. Danilkovitch-Miagkova, and M. A. Leroux, "Concise review: role of mesenchymal stem cells in wound repair," *Stem Cells Transl Med*, vol. 1, no. 2, pp. 142–9, 2012. [Online]. Available: https://www.ncbi.nlm.nih.gov/pubmed/23197761

[14] S. Aggarwal and M. F. Pittenger, "Human mesenchymal stem cells modulate allogeneic immune cell responses," *Blood*, vol. 105, no. 4, pp. 1815–22, 2005. [Online]. Available: https://www.ncbi.nlm.nih.gov/pubmed/15494428

[15] R. Newman, D. Yoo, M. LeRoux, and A. Danilkovitch-Miagkova, "Treatment of inflammatory diseases with mesenchymal stem cells," *Inflammation Allergy - Drug Targets*, vol. 8, no. 2, pp. 110–123, 2009.

[16] A. M. Hocking and N. S. Gibran, "Mesenchymal stem cells: paracrine signaling and differentiation during cutaneous wound repair," *Exp Cell Res*, vol. 316, no. 14, pp. 2213–9, 2010. [Online]. Available: https://www.ncbi.nlm.nih.gov/pubmed/20471978

[17] N. J. Hogrebe and K. J. Gooch, "Direct influence of culture dimensionality on human mesenchymal stem cell differentiation at various matrix stiffnesses using a fibrous self-assembling peptide hydrogel," *J Biomed Mater Res A*, vol. 104, no. 9, pp. 2356–68, 2016. [Online]. Available: https://www.ncbi.nlm.nih.gov/pubmed/27163888

[18] A. M. Hilderbrand, E. M. Ovadia, M. S. Rehmann, P. M. Kharkar, C. Guo, and A. M. Kloxin, "Biomaterials for 4d stem cell culture," *Curr Opin Solid State Mater Sci*, vol. 20, no. 4, pp. 212–224, 2016. [Online]. Available: https://www.ncbi.nlm.nih.gov/pubmed/28717344

[19] M. W. Tibbitt and K. S. Anseth, "Dynamic microenvironments: the fourth dimension," *Sci Transl Med*, vol. 4, no. 160, p. 160ps24, 2012. [Online]. Available: https://www.ncbi.nlm.nih.gov/pubmed/23152326

[20] C. A. DeForest and K. S. Anseth, "Cytocompatible click-based hydrogels with dynamically tunable properties through orthogonal photoconjugation and photocleavage reactions," *Nat Chem*, vol. 3, no. 12, pp. 925–31, 2011. [Online]. Available: https://www.ncbi.nlm.nih.gov/pubmed/22109271

[21] S. R. Caliari, M. Perepelyuk, E. M. Soulas, G. Y. Lee, R. G. Wells, and J. A. Burdick, "Gradually softening hydrogels for modeling hepatic stellate cell behavior during fibrosis regression," *Integr Biol (Camb)*, vol. 8, no. 6, pp. 720–8, 2016. [Online]. Available: https://www.ncbi.nlm.nih.gov/pubmed/27162057

[22] S. P. Zustiak and J. B. Leach, "Hydrolytically degradable poly(ethylene glycol) hydrogel scaffolds with tunable degradation and mechanical properties," *Biomacromolecules*, vol. 11, no. 5, pp. 1348–57, 2010. [Online]. Available: https://www.ncbi.nlm.nih.gov/pubmed/20355705

[23] A. M. Kloxin, A. M. Kasko, C. N. Salinas, and K. S. Anseth, "Photodegradable hydrogels for dynamic tuning of physical and chemical properties," *Science*, vol. 324, no. 5923, pp. 59–63, 2009. [Online]. Available: https://www.ncbi.nlm.nih.gov/pubmed/19342581

[24] R. S. Stowers, S. C. Allen, and L. J. Suggs, "Dynamic phototuning of 3d hydrogel stiffness," *Proc Natl Acad Sci U S A*, vol. 112, no. 7, pp. 1953–8, 2015. [Online]. Available: https://www.ncbi.nlm.nih.gov/pubmed/25646417

[25] A. M. Rosales, C. B. Rodell, M. H. Chen, M. G. Morrow, K. S. Anseth, and J. A. Burdick, "Reversible control of network properties in azobenzene-containing hyaluronic acid-based hydrogels," *Bioconjug Chem*, vol. 29, no. 4, pp. 905–913, 2018. [Online]. Available: https://www.ncbi.nlm.nih.gov/pubmed/29406696

[26] Y. Liang, N. E. Clay, K. M. Sullivan, J. Leong, A. Ozcelikkale, M. H. Rich, M. K. Lee, M. H. Lai, H. Jeon, B. Han, Y. W. Tong, and H. Kong, "Enzyme-induced matrix softening regulates hepatocarcinoma cancer cell phenotypes," *Macromol Biosci*, vol. 17, no. 9, 2017. [Online]. Available: https://www.ncbi.nlm.nih.gov/pubmed/28683186

[27] A. A. Aimetti, M. W. Tibbitt, and K. S. Anseth, "Human neu-trophil elastase responsive delivery from poly(ethylene glycol) hydrogels," *Biomacromolecules*, vol. 10, no. 6, pp. 1484–9, 2009. [Online]. Available: https://www.ncbi.nlm.nih.gov/pubmed/19408953

[28] A. M. Rosales, S. L. Vega, F. W. DelRio, J. A. Burdick, and K. S. Anseth, "Hydrogels with reversible mechanics to probe dynamic cell microenvironments," *Angew Chem Int Ed Engl*, vol. 56, no. 40, pp. 12 132–12 136, 2017. [Online]. Available: https://www.ncbi.nlm.nih.gov/pubmed/28799225

[29] B. D. Cosgrove, K. L. Mui, T. P. Driscoll, S. R. Caliari, K. D. Mehta, R. K. Assoian, J. A. Burdick, and R. L. Mauck, "N-cadherin adhesive interactions modulate matrix mechanosensing and fate commitment of mesenchymal stem cells," *Nat Mater*, vol. 15, no. 12, pp. 1297–1306, 2016. [Online]. Available: https://www.ncbi.nlm.nih.gov/pubmed/27525568

[30] J. C. Grim, T. E. Brown, B. A. Aguado, D. A. Chapnick, A. L. Viert, X. Liu, and K. S. Anseth, "A reversible and repeatable thiol-ene bioconjugation for dynamic patterning of signaling proteins in hydrogels," *ACS Cent Sci*, vol. 4, no. 7, pp. 909–916, 2018. [Online]. Available: https://www.ncbi.nlm.nih.gov/pubmed/30062120

[31] S. B. Anderson, C. C. Lin, D. V. Kuntzler, and K. S. Anseth, "The performance of human mesenchymal stem cells encapsulated in cell-degradable polymer-peptide hydrogels," *Biomaterials*, vol. 32, no. 14, pp. 3564–74, 2011. [Online]. Available: https://www.ncbi.nlm.nih.gov/pubmed/21334063

[32] M. P. Lutolf, J. L. Lauer-Fields, H. G. Schmoekel, A. T. Metters, F. E. Weber, G. B. Fields, and J. A. Hubbell, "Synthetic matrix metalloproteinase-sensitive hydrogels for the conduction of tissue regeneration: engineering cell-invasion characteristics," *Proc Natl Acad Sci U S A*, vol. 100, no. 9, pp. 5413–8, 2003. [Online]. Available: https://www.ncbi.nlm.nih.gov/pubmed/12686696

[33] J. Patterson and J. A. Hubbell, "Enhanced proteolytic degradation of molecularly engineered peg hydrogels in response to mmp-1 and mmp-2," *Biomaterials*, vol. 31, no. 30, pp. 7836–45, 2010. [Online]. Available: https://www.ncbi.nlm.nih.gov/pubmed/20667588

[34] M. C. Giano, D. J. Pochan, and J. P. Schneider, "Controlled biodegradation of self-assembling beta-hairpin peptide hydrogels by proteolysis with matrix metalloproteinase-13," *Biomaterials*, vol. 32, no. 27, pp. 6471–7, 2011. [Online]. Available: https://www.ncbi.nlm.nih.gov/pubmed/21683437

[35] C. N. Salinas and K. S. Anseth, "The enhancement of chondrogenic differentiation of human mesenchymal stem cells by enzymatically regulated rgd functionalities," *Biomaterials*, vol. 29, no. 15, pp. 2370–7, 2008. [Online]. Available: https://www.ncbi.nlm.nih.gov/pubmed/18295878

[36] K. N. Plunkett, K. L. Berkowski, and J. S. Moore, "Chymotrypsin responsive hydrogel: application of a disulfide exchange protocol for the preparation of methacrylamide containing peptides," *Biomacromolecules*, vol. 6, no. 2, pp. 632–7, 2005. [Online]. Available: https://www.ncbi.nlm.nih.gov/pubmed/15762623

[37] A. N. Wilson, R. Salas, and A. Guiseppi-Elie, "Bioactive hydrogels demonstrate mediated release of a chromophore by chymotrypsin," *J Control Release*, vol. 160, no. 1, pp. 41–7, 2012. [Online]. Available: https://www.ncbi.nlm.nih.gov/pubmed/22410116

[38] A. A. Aimetti, A. J. Machen, and K. S. Anseth, "Poly(ethylene glycol) hydrogels formed by thiol-ene photopolymerization for enzyme-responsive protein delivery," *Biomaterials*, vol. 30, no. 30, pp. 6048–54, 2009. [Online]. Available: https://www.ncbi.nlm.nih.gov/pubmed/19674784

[39] R. S. Ashton, A. Banerjee, S. Punyani, D. V. Schaffer, and R. S. Kane, "Scaffolds based on degradable alginate hydrogels and poly(lactide-co-glycolide) microspheres for stem cell culture," *Biomaterials*, vol. 28, no. 36, pp. 5518–25, 2007. [Online]. Available: https://www.ncbi.nlm.nih.gov/pubmed/17881048

[40] K. W. Clancy, J. A. Melvin, and D. G. McCafferty, "Sortase transpeptidases: insights into mechanism, substrate specificity, and inhibition," *Biopolymers*, vol. 94, no. 4, pp. 385–96, 2010. [Online]. Available: https://www.ncbi.nlm.nih.gov/pubmed/20593474

[41] X. Huang, A. Aulabaugh, W. Ding, B. Kapoor, L. Alksne, K. Tabei, and G. Ellestad, "Kinetic mechanism of staphylococcus aureus sortase srta," *Biochemistry*, vol. 42, no. 38, pp. 11 307–15, 2003. [Online]. Available: https://www.ncbi.nlm.nih.gov/pubmed/14503881

[42] H. Hirakawa, S. Ishikawa, and T. Nagamune, "Ca2+ -independent sortase-a exhibits high selective protein ligation activity in the cytoplasm of escherichia coli," *Biotechnol J*, vol. 10, no. 9, pp. 1487–92, 2015. [Online]. Available: https://www.ncbi.nlm.nih.gov/pubmed/25864513

[43] N. Broguiere, F. A. Formica, G. Barreto, and M. Zenobi-Wong, "Sortase a as a cross-linking enzyme in tissue engineering," *Acta Biomater*, vol. 77, pp. 182–190, 2018. [Online]. Available: https://www.ncbi.nlm.nih.gov/pubmed/30006315

[44] I. Chen, B. M. Dorr, and D. R. Liu, "A general strategy for the evolution of bond-forming enzymes using yeast display," *Proc Natl Acad Sci U S A*, vol. 108, no. 28, pp. 11 399–404, 2011. [Online]. Available: https://www.ncbi.nlm.nih.gov/pubmed/21697512

[45] M. W. Popp, J. M. Antos, G. M. Grotenbreg, E. Spooner, and H. L. Ploegh, "Sortagging: a versatile method for protein labeling," *Nat Chem Biol*, vol. 3, no. 11, pp. 707–8, 2007. [Online]. Available: https://www.ncbi.nlm.nih.gov/pubmed/17891153

[46] Z. Wu, X. Guo, and Z. Guo, "Sortase a-catalyzed peptide cyclization for the synthesis of macrocyclic peptides and glycopeptides," *Chem Commun (Camb)*, vol. 47, no. 32, pp. 9218–20, 2011. [Online]. Available: https://www.ncbi.nlm.nih.gov/pubmed/21738926

[47] E. Cambria, K. Renggli, C. C. Ahrens, C. D. Cook, C. Kroll, A. T. Krueger, B. Imperiali, and L. G. Griffith, "Covalent modification of synthetic hydrogels with bioactive proteins via sortase-mediated ligation," *Biomacromolecules*, vol. 16, no. 8, pp. 2316–26, 2015. [Online]. Available: https://www.ncbi.nlm.nih.gov/pubmed/26098148

[48] J. Valdez, C. D. Cook, C. C. Ahrens, A. J. Wang, A. Brown, M. Kumar, L. Stockdale, D. Rothenberg, K. Renggli, E. Gordon, D. Lauffenburger, F. White, and L. Griffith, "On-demand dissolution of modular, synthetic extracellular matrix reveals local epithelial-stromal communication networks," *Biomaterials*, vol. 130, pp. 90–103, 2017. [Online]. Available: https://www.ncbi.nlm.nih.gov/pubmed/28371736

[49] S. A. Fisher, A. E. G. Baker, and M. S. Shoichet, "Designing peptide and protein modified hydrogels: Selecting the optimal conjugation strategy," *J Am Chem Soc*, vol. 139, no. 22, pp. 7416–7427, 2017. [Online]. Available: https://www.ncbi.nlm.nih.gov/pubmed/28481537

[50] M. R. Arkenberg and C. C. Lin, "Orthogonal enzymatic reactions for rapid crosslinking and dynamic tuning of peg-peptide hydrogels," *Biomater Sci*, vol. 5, no. 11, pp. 2231–2240, 2017. [Online]. Available: https://www.ncbi.nlm.nih.gov/pubmed/28991963

[51] M. R. Arkenberg, D. M. Moore, and C. C. Lin, "Dynamic control of hydrogel crosslinking via sortase-mediated reversible transpeptidation," *Acta Biomaterialia*, vol. 83, pp. 83–95, 2019. [Online]. Available: https://www.ncbi.nlm.nih.gov/pubmed/30415064

[52] B. D. Fairbanks, M. P. Schwartz, A. E. Halevi, C. R. Nuttelman, C. N. Bowman, and K. S. Anseth, "A versatile synthetic extracellular matrix mimic via thiol-norbornene photopolymerization," *Adv Mater*, vol. 21, no. 48, pp. 5005–5010, 2009. [Online]. Available: https://www.ncbi.nlm.nih.gov/pubmed/25377720

[53] B. D. Fairbanks, M. P. Schwartz, C. N. Bowman, and K. S. Anseth, "Photoinitiated polymerization of peg-diacrylate with lithium phenyl-2,4,6-trimethylbenzoylphosphinate: polymerization rate and cytocompatibility," *Biomaterials*, vol. 30, no. 35, pp. 6702–7, 2009. [Online]. Available: https://www.ncbi.nlm.nih.gov/pubmed/19783300

[54] C. P. Guimaraes, M. D. Witte, C. S. Theile, G. Bozkurt, L. Kundrat, A. E. M. Blom, and H. L. Ploegh, "Site-specific c-terminal and internal loop labeling of proteins using sortase-mediated reactions," *Nature Protocols*, vol. 8, p. 1787, 2013. [Online]. Available: https://doi.org/10.1038/nprot.2013.101

[55] S. R. Lustig and N. A. Peppas, "Solute diffusion in swollen membranes. ix. scaling laws for solute diffusion in gels," *Journal of Applied Polymer Science*, vol. 36, no. 4, pp. 735–747, 1988.

[56] J. Yang, R. Yan, A. Roy, D. Xu, J. Poisson, and Y. Zhang, "The i-tasser suite: protein structure and function prediction," *Nat Methods*, vol. 12, no. 1, pp. 7–8, 2015. [Online]. Available: https://www.ncbi.nlm.nih.gov/pubmed/25549265

[57] L. A. Solchaga, K. Penick, J. D. Porter, V. M. Goldberg, A. I. Caplan, and J. F. Welter, "Fgf-2 enhances the mitotic and chondrogenic potentials of human adult bone marrow-derived mesenchymal stem cells," *J Cell Physiol*, vol. 203, no. 2, pp. 398–409, 2005. [Online]. Available: https://www.ncbi.nlm.nih.gov/pubmed/15521064

[58] C. C. Lin, C. S. Ki, and H. Shih, "Thiol-norbornene photo-click hydrogels for tissue engineering applications," *J Appl Polym Sci*, vol. 132, no. 8, 2015. [Online]. Available: https://www.ncbi.nlm.nih.gov/pubmed/25558088

[59] J. Van Hoorick, P. Gruber, M. Markovic, M. Rollot, G. J. Graulus, M. Vagenende, M. Tromayer, J. Van Erps, H. Thienpont, J. C. Martins, S. Baudis, A. Ovsianikov, P. Dubruel, and S. Van Vlierberghe, "Highly reactive thiol-norbornene photo-click hydrogels: Toward improved processability," *Macromol Rapid Commun*, vol. 39, no. 14, p. e1800181, 2018. [Online]. Available: https://www.ncbi.nlm.nih.gov/pubmed/29888495

[60] M. Raeeszadeh-Sarmazdeh, R. Parthasarathy, and E. T. Boder, "Fine-tuning sortase-mediated immobilization of protein layers on surfaces using sequential deprotection and coupling," *Biotechnol Prog*, vol. 33, no. 3, pp. 824–831, 2017. [Online]. Available: https://www.ncbi.nlm.nih.gov/pubmed/28218499